Bioorganic Chemistry 157 (2025) 108270

Contents lists available at ScienceDirect

Bioorganic Chemistry

journal homepage: www.elsevier.com/locate/bioorg

Elucidating the therapeutic efficacy of polyherbal formulation for the management of diabetes through endogenous pancreatic β-cell regeneration

Abhijit Sahu [a,b], Pravash Ranjan Mishra [b], Pratyush Pragyandipta [a], Srichandan Rath [a], Ashirbad Nanda [c], Satish Kanhar [c], Dibya Ranjan Sahoo [a], Eeshara Naik [a], Deepali Naik [a], Pradeep K. Naik [a,*]

[a] DBT BUILDER, Govt. of India, Department of Biotechnology and Bioinformatics, Sambalpur University, Jyoti Vihar, Sambalpur, Odisha, India
[b] Department of Anatomy, All India Institute of Medical Sciences (AIIMS), Bhubaneswar, Odisha, India
[c] School of Pharmacy and Life Sciences, Centurion University of Technology and Management, Jatani, Khurda, Odisha, India

ARTICLE INFO

Keywords:
Diabetes
Polyherbal formulation
UHPLCQ-TOF-MS
Glucose uptake
Molecular docking
β-Cells

ABSTRACT

Diabetes mellitus is characterized by the progressive loss of pancreatic β-cells. Owing to the adverse side effects of conventional antidiabetic, ethnopharmacological agents have emerged as adjunct therapies for their management. The present study aims to validate the antidiabetic activity of an aqueous polyherbal extract (APE) via *in silico*, *in vitro*, and *in vivo* models.

UHPLC–Q-TOF-MS and HPLC analysis of APE were performed to identify bioactive secondary plant metabolites. *In silico* approaches implemented to predict the binding efficacy of the active phytoconstituents. Biochemical estimation, antioxidant activity, and *in vitro* and *in vivo* antidiabetic activities of APE were performed. Histomorphological and immunohistological studies of the pancreatic islets were carried out in diabetic animals for microarchitectural study.

UHPLC-Q-TOF-MS identified a total of 60 compounds in APE, of which 39 were reported to have antidiabetic activity, and 16 marker compounds were identified via high-performance liquid chromatography (HPLC). An *in silico* study revealed a strong interaction of verbacoside B with the target proteins. APE is characterized by high flavonoid and phenolic contents with strong antioxidant properties. In *an* in vitro enzymatic assay, APE significantly inhibited α-amylase and α-glucosidase enzymes, with calculated IC_{50} values of 54.26 ± 0.14 and 26.47 ± 0.12 μg/ml, respectively. An *in vitro* glucose uptake assay revealed increased uptake with APE treatment in a dose-dependent manner. APE significantly decreased blood glucose and HbA1c levels and had no side effects on liver or kidney function, as measured from blood parameters. Immunohistological observation revealed 47% regeneration of pancreatic β-cells with APE treatment in diabetic animals.

1. Introduction

Diabetes mellitus (DM) is a group of metabolic ailments characterized by hyperglycemic (elevated blood glucose level) conditions due to abnormal function of the pancreas. India has become the diabetic capital of the world, contributing approximately 77 million cases and 2.2 million deaths annually. This alarming incidence rate underscores the growing concern over the diabetes epidemic in the country, highlighting the significant public health challenge [1]. The islets of Langerhans play important roles in glucose homeostasis [2,3] and include 60–70 % β-cells (insulin-producing), 15–20 % α-cells (glucagon-producing), and the remaining 10–20 % are pancreatic polypeptides (pp-cells), δ cells, and ε-cells [4,5]. The mantle-core architecture of islets enhances insulin secretion via paracrine effects [6,7]. Dysfunction/destruction of pancreatic β-cells leads to an imbalance in glucose homeostasis [8], which subsequently disturbs postprandial blood glucose and HbA1c levels, which is crucial in diabetes management. Despite the introduction of new antidiabetic agents, prolonged use leads to several adverse side effects, including neuropathy, retinopathy, cardiovascular complications, and gastrointestinal complications. These drugs address only

* Corresponding author at: Department of Biotechnology & Bioinformatics, Sambalpur University, Jyoti Vihar, Sambalpur, Odisha 768019, India.
E-mail address: pknaik1973@gmail.com (P.K. Naik).

https://doi.org/10.1016/j.bioorg.2025.108270
Received 29 November 2024; Received in revised form 1 February 2025; Accepted 10 February 2025
Available online 14 February 2025

Table 1
Composition of the polyherbal formulation and the parts used.

Sl no	Plant name	Plant part used	References
1.	*Tinospora cordifolia* (Willd.)	Stem	[14]
2.	*Mangifera indica* L.	Seed	[15]
3.	*Syzygium cumini* (L.)	Bark	[15]
4.	Terminalia arjuna (Roxb. Ex DC.)	Bark	[14,15]
5.	*Curcuma longa* L.	Rhizome	[15]
6.	*Ailanthus excelsa* Roxb.	Leaf	[15]
7.	*Caesalpinia bonduc* L. (Roxb.)	Seed	[17]
8.	*Swertia chirayita* (Roxb.)	Stem	[16]
9.	*Holarrhena pubescens* wall. Ex G. Don	Root	[15]
10.	*Azadirachta indica* A.Juss.	Leaf	[16]
11.	*Murraya koenigii* (L.) Spreng.	Leaf	[14]
12.	*Withania coagulans*	Flower	[17]
13.	*Salacia oblonga* wall. Ex Wight & Arn.	Root	[14]
14.	*Cedrus deodara* (Roxb. Ex D. Don)	Bark	[17]
15.	Picrorhiza kurroa Royle ex Benth.	Root	[14]
16.	*Pterocarpus marsupium* Roxb.	Bark	[14]

the primary clinical symptoms rather than the pathophysiological mechanism of diabetes [9,10].

Recent research on diabetes revealed a chance of endogenous pancreatic β-cell regeneration via the differentiation of induced pluripotent stem cells (iPSCs) into new pancreatic β-cells, islet transplantation, and modifications of other pancreatic cell subtypes to β-cells to mitigate diabetes symptoms. However, these treatment strategies have failed in many diabetic models [11]. Many polyherbal formulations were developed earlier by different groups, and some of them have been approved for the management of diabetes. For example, Madhurakshak Activ, a polyherbal formulation developed by the Dabur Research Foundation, has been tested to increase the rate of glucose absorption and uptake with increasing concentrations via *in vitro* and *in silico* approaches. Another polyherbal formulation (F6-SMONSECCE) has been shown to inhibit the α-amylase enzyme and significantly decrease blood glucose levels and lipid profiles in an alloxan-induced animal model. Similarly, a polyherbal formulation, Ayush 64, was developed and approved by the Ministry of Ayush, Govt. of India for managing diabetes [12,13]. The data collected from ethnological sources, folklore, and traditional healers at Gandhamardhan hill (Bargarh district) provide hope for mitigating diabetic complications in this unventured area. An alternative antidiabetic medication with high efficacy and minimal side effects is needed to overcome the current challenges. In the present study, we developed a polyherbal formulation comprising sixteen selected medicinal plants (Table 1) on the basis of a literature review on ethnobotany and traditional uses of these plants for the management of diabetes to achieve improved therapeutic outcomes without any adverse effects [14–17]. All these plant materials were collected from the wild in different months/seasons on the basis of their availability. This study highlights a folklore medicine (polyherbal formulation) with antioxidant and antidiabetic activities and its ability to modulate insulin-secreting cells in *in silico, in vitro,* and *in vivo* diabetic models.

2. Materials & methods

2.1. Chemicals and reagents

The chemicals used in the present study, including α-amylase, α-glucosidase, alloxan, metformin, acarbose, TPTZ, and ABTS, were purchased from Sigma Aldrich, USA. 2,2-Diphenyl-1-picrylhydrazyl (DPPH), gallic acid, and ascorbic acid were obtained from Himedia, India. LC–MS-grade solvents such as acetonitrile and water were obtained from Avantor, J.T. Baker, Germany. LC–MS-grade reagents such as formic acid, culture media (DMEM), DMSO, MTT, and 2-NBDG were procured from Thermo Fisher Scientific, USA, and ammonium formate was obtained from VWR, Germany. Deionized water was purified with a Milli-Q system (Millipore, USA).

2.2. Plant material and development of powder polyherbal formulations

We prepared a powder polyherbal formulation by mixing equal proportions of different plant parts from 16 different plants followed by aqueous extraction to obtain a polyherbal aqueous extract for evaluating its efficacy against diabetes. All 16 medicinal plants (Table 1), on the basis of traditional knowledge and the literature, are known for their antidiabetic potential. Therefore, we selected these plants, collected their plant parts from Gandhamardhan Hill, Bargarh District, Odisha, India, and blended them in equal proportions to maintain a balanced formulation and ensure synergistic interactions [18] for the preparation of a powder polyherbal formulation. The shed-dried materials were powdered individually with a versatile pulverizer (B.D. instruments) and passed through a sieve of mesh size ASTM 40# for uniform particle size. The sieved plant material was weighed individually to approximately 50 g each, transferred to an octagonal blender (Cijen Pharma, Gujrat) with a 1 kg vessel capacity and mixed at 15 RPM for 20 min. The blend was further removed from the vessel and stored in an airtight container for further use.

Preparation of Polyherbal Aqueous Extract for Phytochemical Analysis and Activity Studies

A quantity of 800 g of the polyherbal powder formulation was subjected to hot aqueous extraction in a Soxhlet apparatus (OMSONS, Germany). The plant material was placed inside a thimble and kept in a 1-L extractor. The extractor was fitted to a round bottom flask (3 l) containing 1.5 l of distilled water. The apparatus was placed on a heating mantle, and the temperature was set at 100 °C for the formation of steam, followed by its condensation using a chiller (Heidolph, Germany). The single siphon cycle was about 90 min, and the process was continued for 72 h to collect the saturated solution in the flask. This process was subsequently repeated two times with 1.5 l of distilled water for 72 h each time for better extraction of phytochemicals from the plant samples [19]. In addition, heat-based extraction methods such as decoctions align with traditional medicine practices and are effective for extracting therapeutic compounds. The polyherbal aqueous extract was dried using a lyophilizer (Svl, SVFD 501 M), and the % yield was 11.25 % (90 g of dried extract).

2.3. Analytical analysis of APE

2.3.1. Ultra-high-performance liquid chromatography-quadrupole time-of-flight mass spectrometry (UHPLCQ-TOF-MS) analysis of APE

UHPLC–Q-TOF-MS analysis of APE was performed on a Xevo G3 QToF Waters Corporation (M.A., USA) equipped with Acquity UPLC I Class Plus and MassLynx software (Waters Corporation, USA). Progenesis Q.I. software (Waters Corporation, USA) was used to analyse the separated compounds. The compounds were separated via an Acquity UPLC HSS T3 column (100 × 2.1 mm × 1.8 µm) (Waters Corporation, USA). The column and sample temperatures were maintained at 40 °C and 15 °C, respectively. The instrumental parameters were set as ionization type of ESI (mode-MS^E), an acquisition time of 25 min with a collision energy of 6 eV (low) and high collision energies of 10–40 eV (ramp) and 10–30 eV for the +ve and –ve modes, respectively. The capillary voltages were set at 3.0 kV for the +ve mode and 2.5 kV for the –ve mode, whereas the cone voltages were set at 40 V for the +ve mode and 30 V for the –ve mode. The source and desolvation temperatures were set at 130 °C and 500 °C, respectively. The cone and desolvation gas flows were maintained at rates of 50 l/h and 750 l/h, respectively. A solution of leucine enkephalin (200 pg/ml, Waters, USA) was infused at a flow rate of 10 µl/min to generate reference ions of *m/z* 556.2771 (M + H, +ve mode) and m/z 554.2615 (M-H, −ve mode). The solvent elution was performed at a flow rate of 0.4 ml/min via a gradient mobile phase (solvent A: 0.1 % formic acid in water and solvent B: 0.1 % formic acid in acetonitrile) for +ve analysis, whereas in –ve mode of analysis, the gradient mobile phase was 1 mM ammonium formate in water (solvent A) and acetonitrile (solvent B). In both modes of analysis, the

volume ratios of solvent B were as follows: 5 % (0–1 min), 5–25 % (1–5 min), 25–35 % (5–8 min), 35–45 % (8–11 min), 45–55 % (11–14 min), 55–90 % (14–20 min), 90–95 % (20–20.1 min), and 100 % (20.1–25 min). The test solution (5 µl) was injected, and the chromatographs were recorded for 25 min.

2.3.2. HPLC profiling of APE

2.3.2.1. Chromatographic conditions. The optimized mobile phase was composed of 0.1 % OPA in water as solvent A and acetonitrile as solvent B in gradient separation mode. The flow rate was maintained at 1.0 ml/min, the sample oven temperature was maintained at 15 °C, and the column oven temperature was maintained at 40 °C. A wavelength of 260 nm was used for detection of the compounds. The major bioactive compounds in the extract of the polyherbal formulation were quantified via an HPLC system (Waters Alliance e2695 separation module with a 2998 photodiode array detector) equipped with Empower Software. The HPLC instrument was organized with a separation module, a quaternary pump, an autosampler, a degasser, a diode array detector and a column oven. Chromatographic separation was carried out using an Exsil Pure 100C-18, 150 × 4.6 mm, 5 µm HPLC column with an injection volume of 10 µl for both the standard and the sample solutions. The gradient elution was carried out with the optimized mobile phase conditions as solvent B (10 % *v*/v) for 2 min in isocratic mode, then increased to B 30 % *v*/v for 15 min in gradient mode, and further increased to 40 % v/v B for 20 min in gradient mode. Solvent B was further increased to 70 % *v*/v for 24 min in gradient mode and maintained at 70 % v/v B for 30 min in isocratic mode. It was further increased to B 90 % v/v for 35 min in gradient mode and maintained at B 90 % v/v for 40 min in isocratic mode. The initial conditions were maintained for 41 min to 45 min, and the concentration of Solvent B was 10 % v/v.

2.3.2.2. Preparation of standard and sample solutions. A standard mixture of 16 standards was accurately weighed, transferred to a 10 ml volumetric flask and diluted with methanol to prepare a concentration of 100 µg/ml. The mixture was sonicated for 15 min until it completely dissolved. Furthermore, the samples were filtered through a 0.45 µm nylon membrane syringe filter before being injected into the chromatographic system. The sample solution was prepared by taking approximately 25 mg of the crude polyherbal formulation extract and transferring it to a 25 ml volumetric flask. The extract was first dissolved in 5 ml of distilled water by sonication for 30 min and further diluted to volume with methanol. The solution was filtered through a 0.45 µm nylon membrane syringe filter before being injected into the chromatographic system.

2.4. Biochemical estimation of APE

2.4.1. Total flavonoid content (TFC)

To estimate the total flavonoid content (TFC) of APE, a reaction mixture of 200 µl of $AlCl_3$ (2 %) and 200 µl of APE (1 mg/ml) was mixed at a 1:1 ratio, followed by incubation at 37 °C for 1 h. To the reaction mixture, 400 µl of distilled water was added, and the absorbance was measured at 420 nm via a spectrophotometer (Shimadzu UV-3600i). Quercetin (1 mg/ml) was used as a control, and a calibration curve was obtained. The TFC was expressed as the dry weight of quercetin (mg/g) [20].

2.4.2. Total phenol content (TPC)

The Folin–Ciocalteu reagent method was utilized to quantify the total phenolic content (TPC) of APE, as reported previously, with slight modifications [20]. APE (0.2 mg/ml) and Folin-Ciocalteu reagent (50 µl) were mixed at a 1:1 ratio, and the reaction mixture was incubated for 10 mins. To the reaction mixture, 50 µl of sodium carbonate solution (20 %) was added to neutralize the mixture, followed by incubation for 30 min at room temperature. The absorbance was measured at 765 nm via a UV–vis spectrophotometer (Shimadzu UV–3600i). Gallic acid (0.1 mg/ml) was used as a standard control. The TPC was expressed as dry-weight gallic acid (GAE).

2.5. In vitro antioxidant analysis of APE

2.5.1. DPPH assay

The antioxidant activity of APE was determined as described previously by utilizing the DPPH assay [21]. DPPH solution (0.03 mg/ml) and APE at various concentrations (20, 40, 60, 80, 100 µg/ml) were prepared. In a test tube, 3 ml of DPPH and 0.1 ml of APE were mixed properly. The reaction mixture was incubated at room temperature for 30 min in the dark. The absorbance was then measured at 517 nm using a spectrophotometer (Shimadzu UV-3600i). Ascorbic acid (1 mg/ml) was used as a standard control. The experiments were carried out in triplicate, and the IC_{50} values were obtained. The following formula was used to calculate % inhibition:

$$\%\text{Inhibition} = [(A_{Con} - A_S)/A_{Con}] \times 100$$

where A_{Con} = the absorbance of the control sample and A_S = the absorbance of the sample.

2.5.2. ABTS radical scavenging assay

The ABTS assay of APE was carried out as described previously with certain modifications [22]. Briefly, the ABTS solution was prepared by adding ABTS (7.4 mM) and potassium persulfate (2.6 mM) at a 1:1 ratio and incubating for 12–16 h in the dark prior to use. Various concentrations (20, 40, 60, 80, and 100 µg/ml) of 0.10 ml APE were mixed with 1.90 ml ABTS solution, and the reaction mixture was incubated for 2 h. The absorbance was then measured at 734 nm via a spectrophotometer (Shimadzu UV–3600i). Ascorbic acid (1 mg/ml) was used as a standard control. The experiments were performed in triplicate, and the results are expressed as the IC_{50} values. The following formula was used to calculate % inhibition:

$$\%\text{Inhibition} = [(A_{Con} - A_S)/A_{Con}] \times 100$$

where A_{Con} = the absorbance of the control sample and A_S = the absorbance of the sample.

2.5.3. Ferric reducing antioxidant power (FRAP) assay

The FRAP assay of APE was carried out as described previously with slight modifications [23]. Briefly, various concentrations of APE (20, 40, 60, 80, 100 µg/ml) and FRAP solution (0.1 M acetate buffer, 10 mM TPTZ, and 20 mM ferric chloride (10:1:1, *v*/v/v)) were prepared. A total of 1.90 ml of FRAP solution was added to 0.10 ml of APE, the reaction mixture was placed in a water bath (37 °C) for 30 min, and the absorbance was measured at 593 nm via a spectrophotometer (Shimadzu UV-3600i). Ascorbic acid (1 mg/ml) was used as a standard control. The experiments were run in triplicate, and the results are expressed as the IC_{50} values. The following formula was used to calculate % inhibition:

$$\%\text{Inhibition} = [(A_{Con} - A_S)/A_{Con}] \times 100$$

where A_{Con} = the absorbance of the control sample and A_S = the absorbance of the sample.

2.6. In silico study

APE contains a variety of bioactive compounds with potential therapeutic effects. Conducting an *in-silico* study allows us to predict which compounds are most likely to interact with key molecular targets, such as IGF-1 receptor kinase and GLUT 4. This helps us elucidate potential mechanisms of action and prioritize compounds for further experimental validation, thereby enhancing our understanding of the efficacy

of the formulation.

2.6.1. Protein preparation

The selected target proteins, IGF-1 receptor kinase and GLUT4, were chosen because of their critical roles in β-cell regeneration, proliferation, and enhanced glucose uptake. The high-resolution X-ray crystallographic structures of both proteins, IGF-1 and GLUT4, with PDB IDs of 1K3A and 7WSM, were selected for the docking experiments. By targeting the IGF-1 receptor kinase, we aimed to explore the mechanisms involved in β-cell survival and regeneration, while the role of the GLUT4 protein in improving cellular glucose uptake through translocation was studied. The downloaded protein structures were subsequently prepared via the Protein Preparation Wizard and Prime tools (Schrödinger, Inc., NY) [24,25], followed by energy minimization (Schrödinger, Inc., NY).

2.6.2. Ligand preparation

The molecular structures of verbascoside B, apigenin 7-apiosyl-glucoside, curcucomosin A, andrographic acid, ricinoleic acid, gymnemic acid I and the standard gliclazide were drawn via Chem-draw. The prepared ligands were imported into the Maestro environment, followed by energy minimization via a Macromodel (Schrödinger-2023, LLC, NY, Release 2023–2 Inc., NY) with the OPLS 2005 force field and PRCG algorithm (energy gradient of 0.001). Geometric optimization was performed via Jaguar (Schrödinger, Inc., NY), and various conformations of the structures were generated via LigPrep (Schrödinger-2023, LLC, NY, Release 2023–2 Inc., NY).

2.6.3. Molecular docking

The prepared ligands were subjected to a blind docking approach due to the nonavailability of cocrystal structures to elucidate the putative binding site for different structures against the insulin-like growth factor 1 (IGF-1) receptor kinase protein and glucose transporter 4 (GLUT 4) protein via the glide algorithm (Schrödinger, Inc., NY). An inner grid box of (12 Å × 12 Å × 12 Å) and an outer grid box (20 Å × 20 Å × 20 Å) were created using the glide grid-receptor generation algorithm (Schrödinger, Inc., NY). Subsequently, glide XP (extra precision) was utilized for docking, and all the docked poses were analysed [26]. The docked conformations of the target protein and ligands were used for the ligand plot. This finding highlights the hydrogen bonding distances and hydrophobic interactions between the ligand and the amino acids at the binding site.

2.6.4. ADME property prediction

A total of 44 absorption, distribution, metabolism, and excretion (ADME) attributes were determined via the QikProp tool (Schrödinger-2023, LLC, NY, Release 2023–2 Inc., NY) for the above-isolated compounds and standard drugs. The acceptability of the compounds was evaluated on the basis of Lipinski's rule of 5 [26].

2.7. In vitro antidiabetic activity of APE

2.7.1. α-Amylase activity

The α-amylase inhibitory activity of APE was determined as described previously [27]. APE (2.5 mg/ml) was mixed with 1 ml of α-amylase (0.02 mg/ml) and incubated at 25 °C for 3 min, after which 1 ml of color reagent (51.961 mol/l) was added, and the mixture was placed in a water bath (B.D. Instruments, LS WB-10P) at 85 °C for 15 min. The mixture was diluted with 9 ml of distilled water, and the absorbance was measured at 540 nm via a spectrophotometer (Shimadzu UV-3600i). Acarbose solution (500 μg/ml) was used as the standard. The percentage of inhibition of α-amylase was calculated via the following formula:

$$\%\text{inhibition} = 100 \times [(A_{Con} - A_{Sm})/A_{Con}]$$

where A_{Con} = the absorbance of the control sample and A_S = the absorbance of the sample.

2.7.2. α-Glucosidase activity

APE (1 mg/ml), phosphate buffer (0.1 mol/l, pH 6.9) and α-glucosidase solution (2.5 mg/ml) were mixed at a ratio of 1:1:1 *v*/v, followed by incubation at 25 °C for 5 min. Then, 100 μl of *p*-nitrophenyl-α-D-glucopyranoside solution (5 mmol/l) was added, and the mixture was further incubated at 25 °C for 10 min. The absorbance was recorded at 405 nm via a spectrophotometer (Shimadzu UV-3600i). Acarbose solution (500 μg/ml) was used as a standard [27]. The percentage of inhibition of α-glucosidase was calculated via the following formula, and the results are expressed as the IC_{50} values:

$$\%\text{inhibition} = 100 \times [(A_{Con} - A_S)/A_{Control}]$$

where A_{Con} = the absorbance of the control sample and A_S = the absorbance of the sample.

2.7.3. Cell culture

The 3T3L1 and MIN6 cell lines were purchased from NCCS Pune and were grown in DMEM (Thermo Fisher) supplemented with 10 % FBS (Gibco) and 1 % penicillin–streptomycin antibiotics (Sigma) at 37 °C and 5 % CO_2 in a humidifier incubator (Eppendorf cell-xpert C170).

2.7.4. Cytotoxicity assay

A 3-(4,5-dimethylthiazol-2-yl)-5-(3-carboxymethoxyphenyl)-2-(4-sulfophenyl)-2H-tetrazolium (MTT) assay was carried out to assess the cytotoxicity of APE in 3T3L1 cells according to previously published methods with slight modifications [28]. Briefly, the cells were seeded in 96-well culture plates ($5 \times 10^{\hat{}}3$ per well) and treated with various concentrations of APE (20, 40, 60, 80, 100, 400, 800 & 1000 μg/ml) at 37 °C and 5 % CO_2 in a humidifier incubator for 48 h. After the incubation period, the media was replaced with 20 μl of MTT (2 mg/ml) and incubated for another 4 h at 37 °C. The absorbance was measured at 490 nm via a microplate reader (Bio-Rad).

2.7.5. Glucose uptake assay

The glucose uptake assay was conducted in the MIN6 cell line via the fluorescent glucose analogue 2-deoxy-2-[(7-nitro-2,1,3-benzoxadiazol-4-yl) amino]-D-glucose (2-NBDG) as previously described [29,30], with slight modifications. Briefly, the cells were seeded at a density of $5 \times 10^{\hat{}}3$ per well in a 96-well culture plate with complete media. The complete media was replaced with glucose-free media for 3 h, followed by treatment with metformin (100 μg/ml) and APE at various concentrations (100, 200, 500, 700, and 1000 μg/ml) for 48 h. After the incubation period, the treated media was replaced with 100 μM 2-NBDG for 2 h, after which the cells were washed in chilled PBS. The absorbance was measured at 535 nm via a microplate reader (Bio-Rad).

2.8. In vivo antidiabetic study

2.8.1. Animal housing

Wistar rats of both sexes (176 ± 15 g) were kept under standard laboratory conditions at room temperature (25 ± 2 °C) with a 12-h L:D cycle for two weeks prior to the start of the experiment. The animals were fed ad libitum with a standard pellet diet and allowed free access to water. After approval was obtained from the Institutional Animal Ethical Clearance (IEAC) of the Department of Biotechnology & Bioinformatics, Sambalpur University, Burla, Odisha, video no. SU/BTBI/IAEC/2023/02, the experiment was conducted.

2.8.2. Acute toxicity

Oral acute toxicity studies were performed as per the Organization for Economic Cooperation and Development guidelines (OECD-423) [31]. The animals were segregated into five groups, with six animals ($n = 6$) in each, and fasted overnight. APE was given orally at single doses of 1000, 2000, 3000, 4000, and 5000 mg/kg b.w. in groups I-V, respectively. After dosing, the animals were observed for an initial 30 min, followed by 4 hr, 24 hr, and, finally, 14 days. Several parameters,

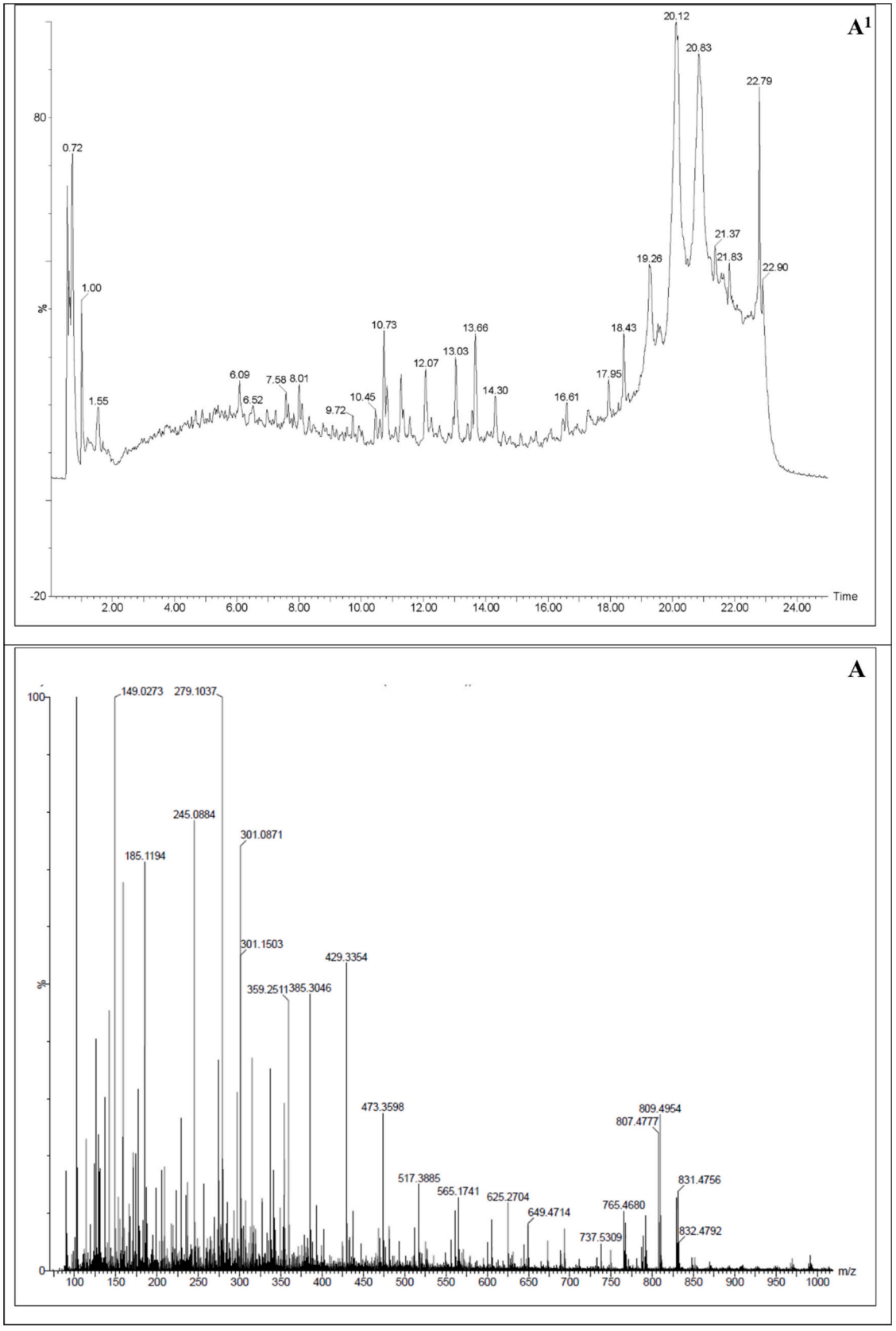

Fig. 1. **A[1].** TIC chromatogram of APE in positive mode **A.** UHPLC-Q-TOF-MS chromatogram of APE in positive mode (37 marker compounds); **B[1].** TIC chromatogram of APE in negative mode **B.** Negative mode (23 marker compounds) was identified on the basis of their respective mass ions, spectral databases, fragmentation patterns, and relevant literature.

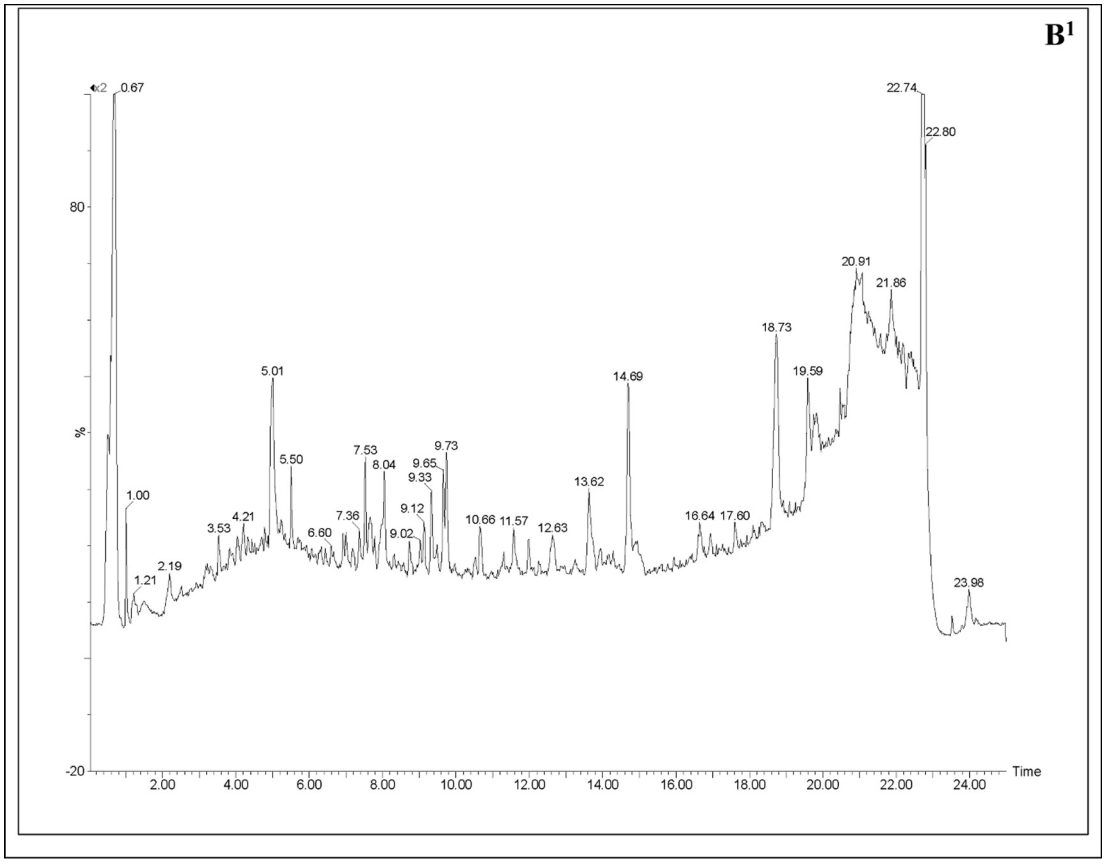

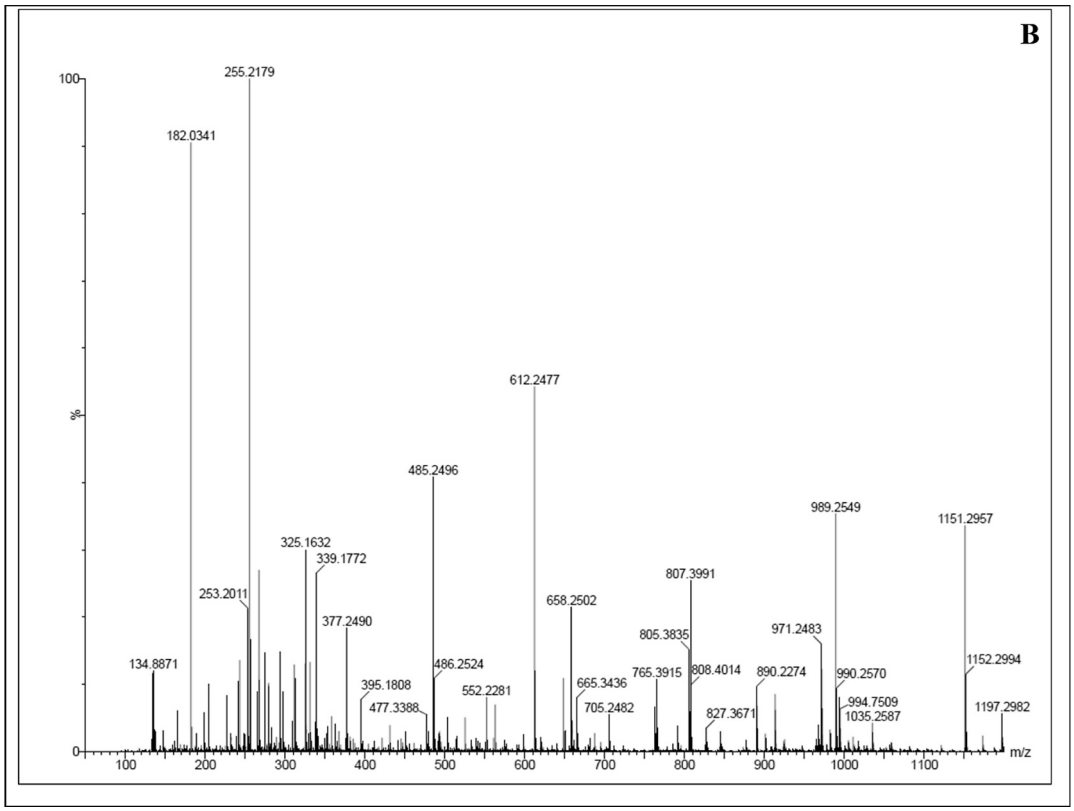

Fig. 1. (*continued*).

Table 2
UHPLC-Q-TOF-MS analysis of APE in both positive and negative modes. A total of 60 different marker compounds were identified on the basis of their respective mass ions, online and offline spectral databases, fragmentation patterns, and relevant literature.

Sl. No.	RT	Compound, Mol formula	Mol wt, m/z	Nature of compound	Biological activity	References
(A) Positive ionization mode analysis of APE						
1	1.55	Gallic acid $C_7H_6O_5$	170.02, 171.0281	Phenolic	Antidiabetic	[55]
2	4.18	Mangiferin $C_{19}H_{18}O_{11}$	422.086, 423.0936	Flavonoid	Antidiabetic	[56]
3	4.28	Noreugenin $C_{10}H_8O_4$	192.0415, 193.0488	Chromone	Antidiabetic	[57]
4	4.43	Litseglutine B $C_{20}H_{23}NO_4$	341.163, 342.1709	Alkaloid	Antidiabetic	[44]
5	4.68	Apigenin 7-apiosyl-glucoside $C_{26}H_{28}O_{14}$	564.148, 565.1561	Flavonoid	Antidiabetic	[54]
6	5.26	Resokaempferol 7-glucoside $C_{21}H_{20}O_{10}$	432.1060, 433.1133	Flavonoid		
7	5.28	Ellagic acid $C_{14}H_6O_8$	302.0066, 303.0139	Polyphenol	Antioxidant antidiabetic	[77]
8	5.50	Ajmaline $C_{20}H_{26}N_2O_2$	326.2000, 327.2073	Alkaloid	Antidiabetic	[78]
9	6.02	Yohimbine $C_{21}H_{26}N_2O_3$	354.1949, 355.2022	Alkaloid	Antidiabetic	[79]
10	6.04	Apigenin 7-glucuronide $C_{21}H_{18}O_{11}$	446.0857, 447.0930	Flavonoid	Antidiabetic	[54]
11	6.14	7-hydroxyeucommic acid $C_9H_{14}O_6$	218.0791, 241.0683	Carboxylic acid		
12	7.58	Andrographolactone $C_{20}H_{24}O_2$	296.1779, 297.1852	Diterpenoid	Antidiabetic	[80]
13	7.66	23-hydroxybetulinic acid $C_{30}H_{48}O_4$	472.3551, 473.3624	Triterpenoid	–	–
14	7.74	7α-hydroxy Campesterol $C_{28}H_{48}O_2$	416.3668, 439.3560	Steroid	–	–
15	7.76	Ar-Turmerone $C_{15}H_{20}O$	216.1513, 217.1586	Sesquiterpenoid	Antidiabetic	[81]
16	7.94	Bonducellpin D $C_{22}H_{28}O_7$	404.1837, 427.1729	Diterpenoid	–	–
17	8.01	(−)-α-curcumene $C_{13}H_{18}$	174.1413, 197.1305	Sesquiterpene	–	–
18	8.01	Caesalpinolide D $C_{20}H_{30}O_4$	334.2135, 335.2208	Diterpene	–	–
19	8.08	Liquiritigenin $C_{15}H_{12}O$	256.0742, 257.0815	Flavonoid	Antidiabetic	[82]
20	8.09	14-deoxy-11,12-didehydroandrographiside $C_{26}H_{38}O_9$	494.2521, 417.2413	Diterpenoid	Antihyperglycemic	[58]
21	8.32	Norcaesalpinin E $C_{21}H_{28}O_6$	376.1896, 399.1788	Diterpenoid		
22	8.54	Isoliquiritigenin 4,4′-diglucoside $C_{27}H_{32}O_{14}$	580.1821, 581.1894	Flavonoid	–	–
23	9.09	Arjunolic acid $C_{30}H_{48}O_5$	488.3507, 489.3580	Triterpenoid	Antidiabetic	[69]
24	9.75	Verbascoside B $C_{21}H_{34}O_{15}$	526.1905, 549.1797	Polyphenol	Antidiabetic	[70]
25	9.92	2,3-dihydro withanolide E $C_{28}H_{40}O_7$	488.2782, 411.2674	Steroid	–	–
26	10.45	Arjungenin $C_{30}H_{48}O_6$	504.3458, 527.3350	Triterpenoid	Antidiabetic	[71]
27	10.73	Curcucomosin A $C_{20}H_{26}O_3$	314.1887, 315.1960	Diterpenoid	–	–
28	10.82	3-O-coumaroyl arjunolic acid $C_{39}H_{54}O_7$	634.3896, 673.3527	Triterpenoid	–	–
29	12.07	β-Hydrojuglone $C_{10}H_8O_3$	176.0466, 177.0539	Phenolic	–	–
30	12.25	9,10,18-trihydroxy octadecanoic acid $C_{18}H_{36}O_5$	332.2566, 355.2458	Hydrocarbon	–	–
31	12.98	Curcumenone $C_{15}H_{22}O_2$	234.1620, 257.1512	Sesquiterpenoid	Antidiabetic	[83]
32	13.03	Gymnemic acid I $C_{43}H_{66}O_{14}$	806.4448, 807.4521	Triterpenoid	Antidiabetic	[72]
33	13.66	Stigmasterol glucoside $C_{35}H_{58}O_6$	574.4256, 597.4148	Steroid	Antidiabetic	[84]
34	13.66	Gymnemic acid ii $C_{43}H_{68}O_{14}$	808.4608, 809.4681	Triterpenoid	Antidiabetic	[72]
35	14.32	9,10-epoxyoctadecanoic acid $C_{18}H_{34}O_4$	314.2460, 337.2352	Hydrocarbon	–	–
36	17.95	Mangiferic acid $C_{18}H_{32}O_2$	280.2403, 281.2476	Fatty acid	Antidiabetic	[85]
37	17.95	Ricinoleic acid $C_{18}H_{34}O_3$	298.2510, 299.2583	Fatty acid	Antidiabetic	[73]
(B) Negative ionization mode analysis of APE						
1	2.49	Ellagic acid 2-rhamnoside $C_{20}H_{16}O_{12}$	448.0642, 447.0569	Polyphenol	Antidiabetic	[86]
2	3.30	5-Feruloylquinic acid $C_{17}H_{20}O_9$	368.1105, 367.1032	Ester	Antidiabetic	[87]
3	3.53	Andrographic acid $C_{20}H_{28}O_6$	364.1881, 363.1808	Carboxylic acid	Antidiabetic	[86]
4	3.55	Isovitexin 6''-O-glucoside $C_{27}H_{30}O_{15}$	594.1586, 593.1513	Flavonoid	Antidiabetic	[53]
5	3.82	Lucidin 3-O-β-primeveroside $C_{26}H_{28}O_{14}$	564.1473, 563.1400	Anthraquinone	–	–
6	4.20	Apigenin 7-glucoside-(2″,3″)-diacetate $C_{25}H_{24}O_{12}$	516.1262, 515.1189	Flavonoid	–	–
7	4.32	Luteolin-5-O-glucoside $C_{21}H_{20}O_{11}$	448.1002, 447.0929	Flavonoid	Antidiabetic	[51]
8	4.43	Apigenin 4′-glucuronide $C_{21}H_{18}O_{11}$	446.0850, 445.0777	Flavonoid	Antioxidant	[88]
9	4.48	14-Acetylandrographolide $C_{22}H_{32}O_6$	392.2200, 391.2127	Diterpenoid	Antidiabetic	[89]
10	4.78	δ-Caesalpin $C_{20}H_{30}O_6$	366.2033, 411.2015	Diterpenoid		
11	4.78	Deacylgymnemic acid $C_{36}H_{58}O_{12}$	682.3930, 681.3857	Triterpenoid	Antidiabetic	[90]
12	5.24	Norcaesalpinin F $C_{21}H_{26}O_7$	390.1679, 435.1661	Diterpenoid	Antidiabetic	[91]
13	7.61	Terminolic acid $C_{30}H_{48}O_6$	504.3452, 503.3380	Triterpenoid	Antidiabetic	[92]
14	7.69	Gymnemic acid iv $C_{41}H_{64}O_{13}$	764.4350,763.4277	Triterpenoid	Antidiabetic	[72]
15	8.06	Gymnemic acid xiii $C_{41}H_{66}O_{13}$	766.4500, 765.4427	Triterpenoid	Antidiabetic	[72]
16	9.65	Neoandrographolide $C_{26}H_{40}O_8$	480.2725,525.2707	Diterpenoid		
17	11.02	Withanolide A $C_{28}H_{38}O_6$	470.2675,469.2603	Steroid	Antidiabetic	[93]
18	11.57	Withanolide F $C_{28}H_{38}O_6$	470.2648,505.2342	Steroid	Antidiabetic	[93]
19	11.64	Withanone $C_{28}H_{38}O_6$	470.2676,469.2603	Triterpenoid	–	–
20	11.98	6-keto stearic acid $C_{18}H_{34}O_3$	298.2506, 297.2433	Fatty acid	–	–
21	14.34	Azadirachtin I $C_{32}H_{42}O_{12}$	618.2655, 617.2582	Hydrocarbon	Antidiabetic	[94]
22	14.98	Myristic acid $C_{14}H_{28}O_2$	228.2084, 227.2011	Fatty acid	Antidiabetic	[95]
23	15.55	Neocaesalpin C $C_{24}H_{34}O_9$	466.2224, 465.2151	Triterpenoid	–	–

including alterations in the skin, fur, and eyes, body weight, and behavioral patterns, were measured. Additionally, the mortality rate was monitored to assess the toxicity of APE. The LD_{50} value was determined according to Litchfield and Wilcoxon's methods [32].

2.8.3. Subacute toxicity

The oral subacute toxicity study was conducted as per OECD guidelines 423 [31]. Briefly, the animals were fasted overnight prior to dosing. The animals were given APE orally at a dose of 500 mg/kg b.w. for four weeks, followed by observation of any clinical symptoms of mortality or changes in the behavioral and physiochemical parameters. Upon completion of the experiment, vital organs, such as the brain, liver, kidney, pancreas, lungs, and heart, were dissected for histopathological observation [33].

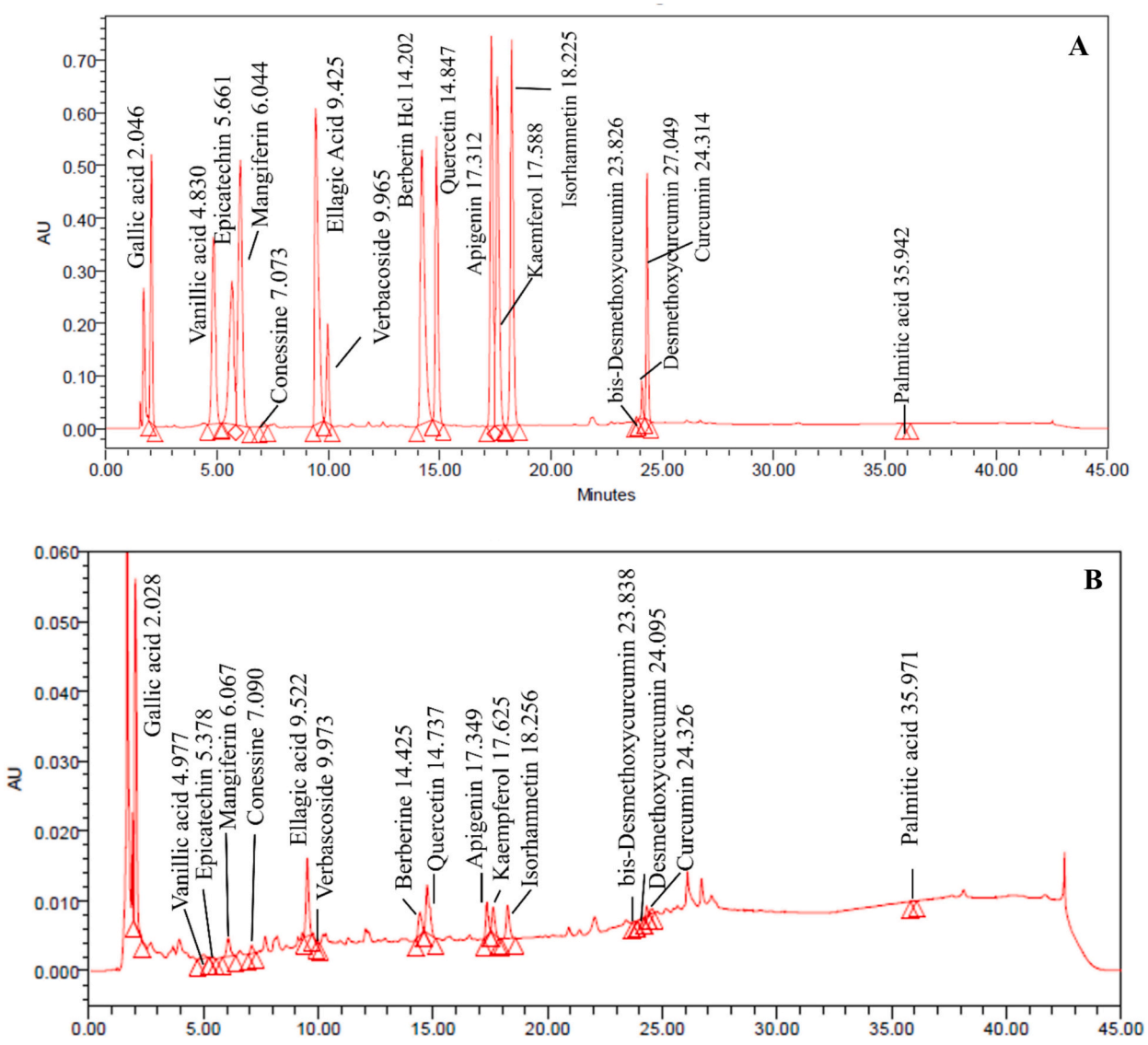

Fig. 2. HPLC chromatograms of the marker compounds on the basis of their mass ions, spectral databases, fragmentation patterns, and relevant literature of standards (A) and APE (B).

2.8.4. Chemical induction of diabetes

The chemical induction of diabetes in the animals was carried out via alloxan following a previously described method, with certain modifications [34]. The present study focused mainly on the function of β-cells in diabetes. Alloxan selectively destroys pancreatic β-cells via the production of reactive oxygen species (ROS), providing a direct model for β-cell destruction. This makes us suitable for investigating whether the developed polyherbal formulation can regenerate lost β-cells. In contrast, the high-fat diet-induced diabetes model primarily induces insulin resistance in peripheral tissues, which is less relevant to studies focused on β-cell regeneration. The animals were fasted overnight and then injected *i.p.* with freshly prepared alloxan (140 mg/kg b.w.). After seven days of induction, the blood glucose levels were measured via a digital blood glucose meter (Accu-Check, India). The animals with blood glucose levels ≥250 mg/dl were considered diabetic and were included in the study [35].

2.8.5. Evaluation of the antidiabetic effect of APE

The selected animals were divided into four groups, with six animals ($n = 6$) in each group. All the treatment groups were administered their respective drugs for four weeks.

Group-I (Normal): fed 0.9 % normal saline.

Group II (diabetic, alloxan-induced): fed 0.9 % normal saline.

Group III (alloxan-induced, metformin-treated): fed metformin (10 mg/kg b.w., p.o.)

Group IV (alloxan-induced, APE-treated): fed APE (500 mg/kg b.w., p.o.)

Every other week, body weight and blood sugar levels were measured until the end of the experiment. At the end of the experiment (on the 29th day), the animals were anaesthetized by mild anaesthesia (isoflurane), followed by cervical dislocation, and blood was collected via cardiac puncture. The serum was separated from the blood (at 5000 rpm for 10 min) to study biochemical parameters, including urea, creatinine (CREA), alanine transaminase (ALT/SGPT), aspartate aminotransferase (AST/SGOT), albumin (ALB), alkaline phosphatase (ALP), cholesterol (CHOL), triglycerides (TG), total protein (TP), high-density lipoprotein (HDL), and insulin, via an automated biochemical analyser (Biovet, Smart-5DX) with their respective standard kits. The pancreatic tissues were collected in 10% neutral buffered formalin (NBF) for histopathological and immunohistochemistry studies.

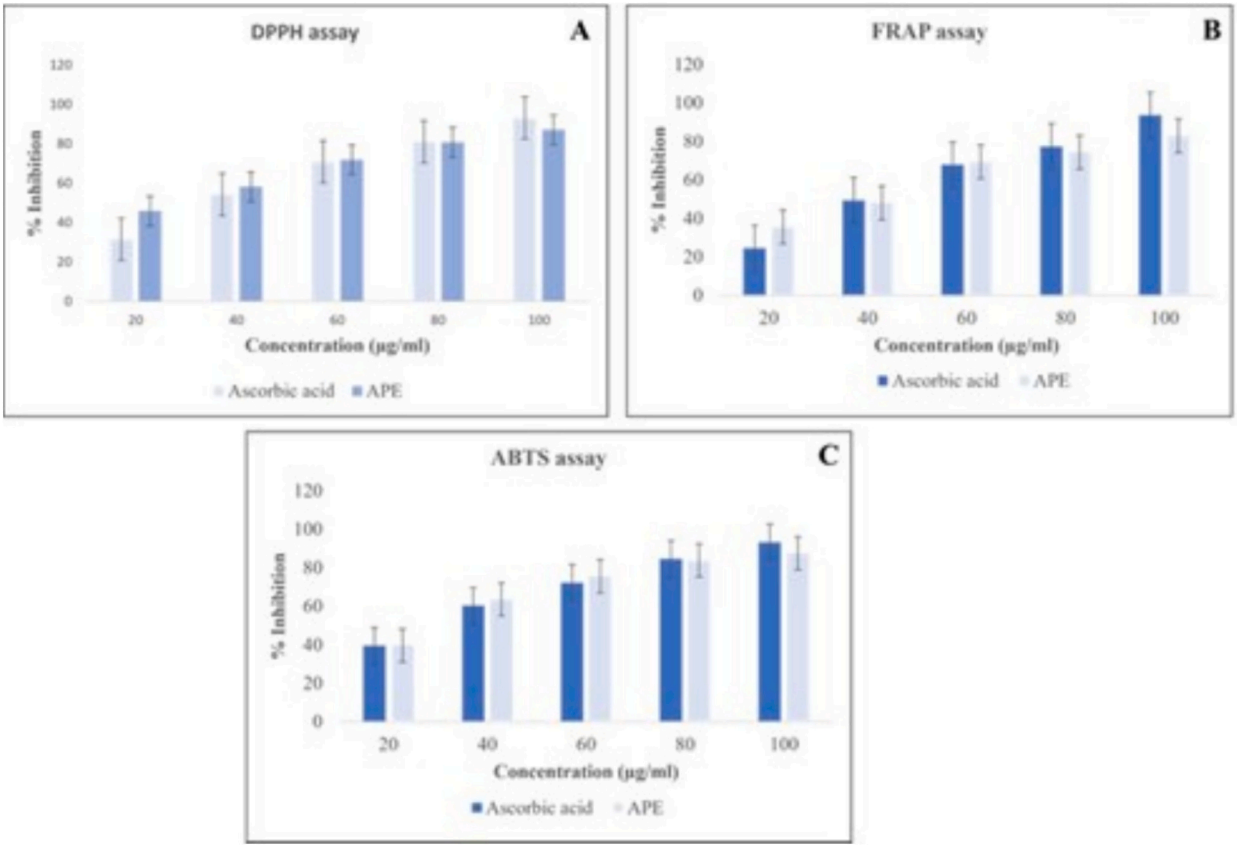

Fig. 3. Free radical scavenging activity of ascorbic acid and APE. A. DPPH, B. FRAP and C. ABTS assays. APE showed strong antioxidant activity, as evidenced by these assays.

2.8.6. Statistical analysis

The data are presented as the mean ± SEM ($n = 6$). Statistical analysis was carried out at $p < 0.05$ between the experimental groups via one-way analysis of variance (ANOVA) followed by Tukey's multiple comparison tests via GraphPad (Prism 9, Graph PAD, USA).

2.8.7. Histopathological and immunohistological studies

For the histopathological study, the collected pancreata were fixed with 10% NBF, dehydrated, rehydrated and embedded in paraffin (Medimas, India). A 4 µm paraffin section was cut and stained with hematoxylin & eosin (H&E) for autolysis features [36]. The tissues with prominent microarchitecture were further subjected to immunohistochemistry (IHC) staining.

IHC staining of 4 µM paraffin sections was performed with the primary antibodies anti-synaptophysin, anti-insulin (Pathnitu, Livermore, California), and anti-glucagon (Bioss Inc., USA) [6]. The prepared slides were examined under a bright field inverted microscope (Nikon eclipse Ts2, Japan) to observe the morphological features and the status of β-cells in the pancreatic islets.

3. Results

3.1. Analytical analysis

3.1.1. UHPLC-Q-TOF-MS analysis of APE

The marker components of APE were identified and validated by utilizing the respective mass ions, spectral databases, fragmentation patterns, and relevant literature. With the use of a full-spectrum scan, data acquisition was carried out in both positive (+ve) and negative (−ve) ionization modes. The chromatogram revealed a total of 60 compounds (37 from the +ve spectrum and 23 from the -ve spectrum), represented by their peak number, RT, molecular formula, compound name, m/z ratio, fragment number, and molecular mass (Table 2). Most of the compounds identified in the APE are known for their antidiabetic activities. The chromatograms of the identified compounds from positive ionization mode are presented in Fig. 1A, and those from negative ionization mode are presented in Fig. 1B. Both chromatograms revealed all the ion peaks, including those of the solvent. Furthermore, the ionization method runs on an MS^E continuum with a collision energy of 6 eV (low) and high collision energies of 10–40 eV (ramp). Hence, it takes even the fragmentation spectra of the molecular ion peakand have been represented in the Table 2. All the masses (m/z) and their fragment ions shown in the table are present in the TIC at their given retention time, with very prominent and sharp peaks when extracted from the TIC.

3.1.2. HPLC profiling of APE

HPLC separation of the 16 bioactive phytochemical constituents was carried out on a C18 column via a gradient elution program with 0.1 % OPA in water as mobile phase A and acetonitrile as mobile phase B at different concentrations. The flow rate was kept constant at 1 ml/min, and the column oven temperature was set at 40 °C. The wavelength was fixed at 260 nm. No interference was observed from the diluents at this detection wavelength in the standard and sample solutions. The 16 sharp peaks were well separated in the standard solution and well identified and quantified in the sample solution (Fig. 2).

3.2. Biochemical estimation APE

3.2.1. Total flavonoid content

The flavonoid content of medicinal plants is a crucial part of interest in drug discovery. Some well-known mechanisms of flavonoids include the inhibition of oxidative enzymes, hydrolytic free radical scavenging

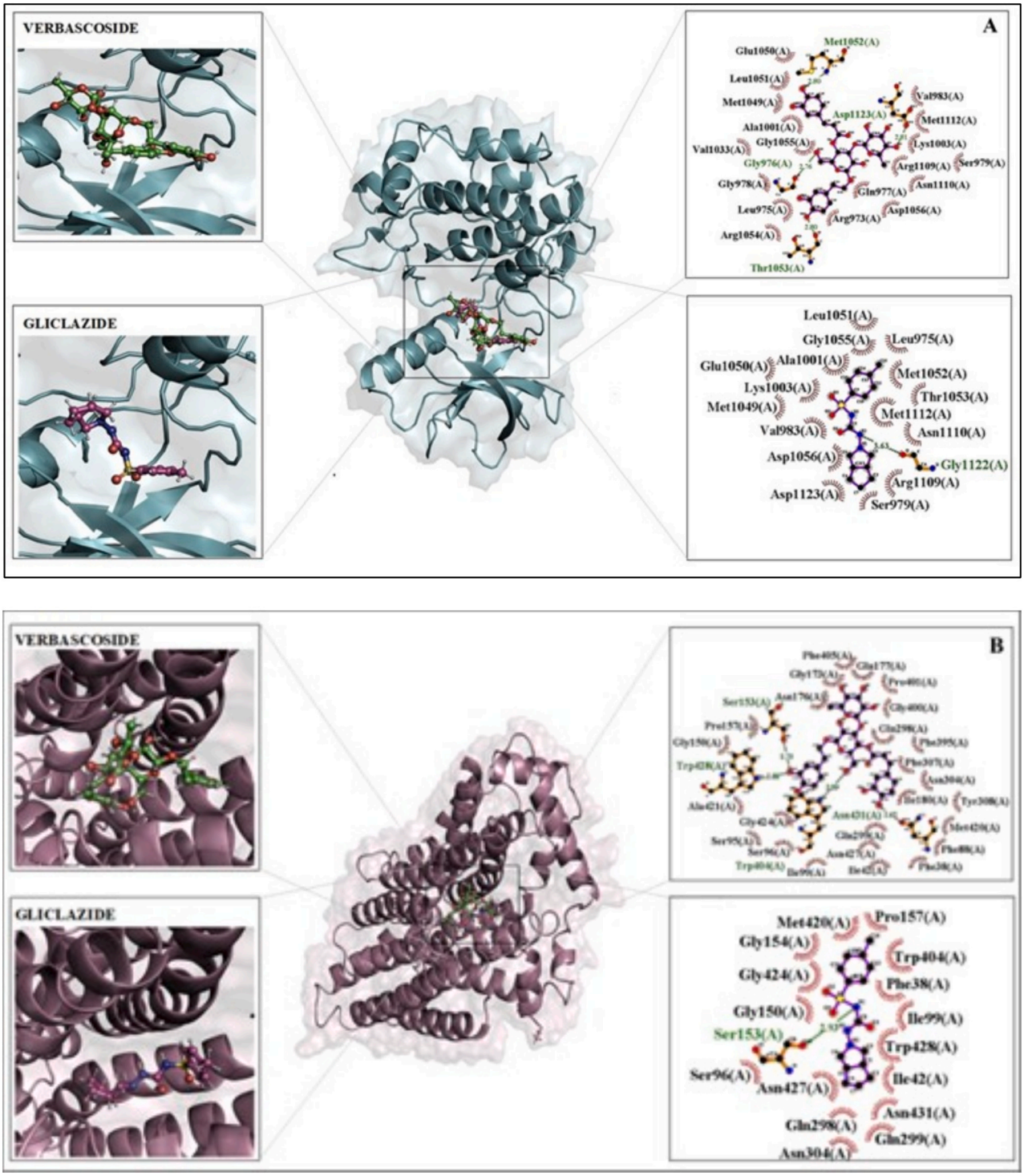

Fig. 4. The verbascoside B compound from APE was well accommodated inside the active binding site of the IGF-I (A) and GLUT4 (B) proteins. The binding site is represented as a macro model surface with cyan color (IGF—I) and purple color (GLUT 4). Ligplot analysis revealed the interaction of amino acid binding sites with verbascoside B and gliclazide. The binding site residues involved in the interactions are slightly different, mainly because of the variation in functional groups. The hydrogen bonds formed are represented as dotted lines. (For interpretation of the references to color in this figure legend, the reader is referred to the web version of this article.)

activity, and anti-inflammatory activity. The total flavonoid content (TFC) of APE was calculated to be 6.465 ± 0.682 mg/Q.E. g D.W. is based on the standard curve of quercetin ($Y = 0.0017\times + 0.002$, $R^2 = 0.9983$).

3.2.2. Total phenol content

Phenol is an abundant secondary metabolite that is found mainly in plants and comprises many biologically active ingredients. These compounds have a variety of biological activities, including anticarcinogenic, antioxidant, and antimutagenic activities. The total phenol content of APE was calculated to be 10.089 ± 1.084 mg/GAE g D.W. on

Table 3
Docking results (Glide XP) of identified compounds from APE with respect to different binding sites of the insulin-like growth factor 1 receptor kinase protein (1K3A) (A) and GLUT4 protein (B) by sitemap (Schrodinger package, 2023–3).

A. Insulin-like growth factor 1 receptor kinase protein (1K3A)

Verbascoside B				
Site ID	**Site score**	**Volume (Å)^3**	**Dscore (Å)^3**	**Glide XP score (kcal/Mol)**
1	1.029	479.257	1.075	−12.433
2	0.846	184.191	0.834	−9.133
3	0.628	131.069	0.599	−9.022
4	0.693	133.298	0.628	−10.602
5	0.650	124.466	0.599	−10.439
Apigenin 7-apiosyl-glucoside				
1	1.029	479.257	1.075	−11.704
2	0.846	184.191	0.834	−6.810
3	0.628	131.069	0.599	−8.996
4	0.693	133.298	0.628	−8.863
5	0.650	124.466	0.599	−8.334
Curcucomosin A				
1	1.029	479.257	1.075	−6.235
2	0.846	184.191	0.834	−2.409
3	0.628	131.069	0.599	−3.742
4	0.693	133.298	0.628	−5.023
5	0.650	124.466	0.599	−3.576
Andrographic acid				
1	1.029	479.257	1.075	−5.712
2	0.846	184.191	0.834	−4.106
3	0.628	131.069	0.599	−4.010
4	0.693	133.298	0.628	−5.198
5	0.650	124.466	0.599	−5.335
Ricinoleic acid				
1	1.029	479.257	1.075	−6.190
2	0.846	184.191	0.834	−1.473
3	0.628	131.069	0.599	−1.846
4	0.693	133.298	0.628	−1.858
5	0.650	124.466	0.599	−4.348
Gymnemic acid I				
1	1.029	479.257	1.075	−7.682
2	0.846	184.191	0.834	−6.610
3	0.628	131.069	0.599	−6.403
4	0.693	133.298	0.628	−7.831
5	0.650	124.466	0.599	−8.637
Gliclazide (standard)				
1	1.029	479.257	1.075	−2.605
2	0.846	184.191	0.834	−2.048
3	0.628	131.069	0.599	−0.791
4	0.693	133.298	0.628	−2.067
5	0.650	124.466	0.599	−1.301

B. GLUT4 protein

Verbascoside B				
Site ID	**Site score**	**Volume (Å)^3**	**Dscore (Å)^3**	**Glide XP score (kcal/Mol)**
1	1.091	1402.827	1.131	−17.825
2	1.023	456.276	1.093	−12.033
3	1.037	217.376	1.019	−10.841
4	0.834	160.524	0.877	−9.788
5	0.899	73.316	0.954	−3.254
Apigenin 7-apiosyl-glucoside				
1	1.091	1402.827	1.131	−15.042
2	1.023	456.276	1.093	−10.676
3	1.037	217.376	1.019	−7.587
4	0.834	160.524	0.877	−6.749
5	0.899	73.316	0.954	−3.347
Curcucomosin A				
1	1.091	1402.827	1.131	−8.017
2	1.023	456.276	1.093	−4.808
3	1.037	217.376	1.019	−3.786
4	0.834	160.524	0.877	−4.330
5	0.899	73.316	0.954	−3.607
Andrographic acid				
1	1.091	1402.827	1.131	−7.367
2	1.023	456.276	1.093	−4.505
3	1.037	217.376	1.019	−5.806
4	0.834	160.524	0.877	−3.447
5	0.899	73.316	0.954	−4.930
Ricinoleic acid				
1	1.091	1402.827	1.131	−5.420
2	1.023	456.276	1.093	−3.841
3	1.037	217.376	1.019	−2.416
4	0.834	160.524	0.877	−3.590
5	0.899	73.316	0.954	−1.494
Gymnemic acid I				
1	1.091	1402.827	1.131	−12.090
2	1.023	456.276	1.093	−6.674
3	1.037	217.376	1.019	−8.132
4	0.834	160.524	0.877	−6.326
5	0.899	73.316	0.954	
Gliclazide (standard)				
1	1.091	1402.827	1.131	−3.332
2	1.023	456.276	1.093	−2.568
3	1.037	217.376	1.019	−3.219
4	0.834	160.524	0.877	−1.602
5	0.899	73.316	0.954	−2.868

the basis of the standard curve of gallic acid ($Y = 0.0099\times + 0.1245$, $R^2 = 0.9861$).

3.3. In vitro antioxidant analysis of APE

3.3.1. DPPH free radical scavenging assay

DPPH radical scavenging activity provides a reliable, quantitative, and comparative measure of antioxidant activity and is widely used to evaluate antioxidant activity. The antioxidant activity (DPPH) of APE, expressed as the IC_{50} value, was 24.15 μg/ml, which is less than the IC_{50} of ascorbic acid (38.42 μg/ml) (Fig. 3 A).

3.3.2. ABTS radical scavenging assay

ABTS is a versatile and quantitative method for assessing the antioxidant capacity of plant extracts. This assay helps to identify and standardize the therapeutic potential of the extract. The calculated IC_{50} value of APE was found to be 25.485 μg/ml, which is comparable with that of standard ascorbic acid (IC_{50} value of 29.702 μg/ml) (Fig. 3 B).

3.3.3. Ferric reducing antioxidant power (FRAP) assay

Antioxidants are multifaceted processes that are mediated by several mechanisms and are influenced by many factors. In the present study, we used a reducing power assay (FRAP) to understand the different mechanisms of APE. The IC_{50} value for APE was calculated to be 39.95 μg/ml, which was comparable with the standard ascorbic acid value of 44.87 μg/ml (Fig. 3 C).

3.4. In silico study

3.4.1. Molecular docking study

Among all the selected compounds, verbascoside B exhibited the highest binding affinity for both the insulin-like growth factor 1 receptor kinase protein and the GLUT 4 protein, with docking scores of −12.433 and −17.825 kcal/mol, respectively, while the standard drugs subsequently had binding affinities of −2.605 and -3.332 kcal/mol, respectively. These sites were considered potential binding sites for the compound. Furthermore, the binding modes of these compounds were visualized with Ligplot (Fig. 4 A & B). The binding of verbascoside B with the insulin-like growth factor 1 receptor kinase protein involves four hydrogen bonds with Gly A976, Met A1052, Thr A1053, and Asp A1123, and the binding with GLUT 4 also involves four hydrogen bonds with Ser A153, Trp A404, Trp A428, and Asn A431. The standard

Table 4
QikProp (Schrodinger package, 2023–3) was used to determine the ADME properties of verbascoside B and the standard gliclazide. These molecules are associated with all the ADME parameters.

Sl no	ADME screening	Verbascoside B	Gliclazide	Recommended Values
1	Mw.	624.59	323.40	130–725
2	SASA	949.37	657.31	300–1000
3	Accpt HB	20.30	5.00	2.0–20.0
4	QPpolrz	53.15	36.70	13.0–70.0
5	QPlogPoct	42.14	16.11	8.0–35
6	QPlogPw	35.14	9.53	4.0–45.0
7	QPlogPo/w	−1.55	2.64	−2.0-6.5
8	QPlogHERG	−6.91	−4.39	Below −5.0 < 25 poor
9	QPPCaco	1.52	512.03	> 500 greats
10	QPlogBB	−5.55	−1.02	−3.0-1.2 < 25 poor
11	QPPMDCK	0.44	291.70	>500 great
12	QPlogKp	−6.15	−3.10	−8.0- -1.0
13	QPlogKhsa	−1.47	0.13	−1.5-1.5
14	Rule of five (no. of violations)	3	0	Maximum is 4

reference drug gliclazide bound to the insulin-like growth factor 1 receptor kinase protein and GLUT4 protein and exhibited only one hydrogen bond with Gly A1112 and Ser A153, respectively. Moreover, the interactions of these compounds with the binding site residues revealed substantial hydrophobic interactions. The docking scores of the selected compounds are collated in Table 3.

3.4.2. ADME property prediction

Lipinski's rule for five methods was used to assess the desirability of verbascoside B and standard drugs as vital drugs. The value of verbascoside B was considerable for each characteristic evaluated, and every drug-like capability was validated according to Lipinski's rule of five (Table 4).

3.5. In vitro antidiabetic assay

3.5.1. Enzyme inhibition assay

The antidiabetic potential of APE was evaluated via α-amylase and α-glucosidase inhibition assays. APE showed promising antidiabetic activity by inhibiting both enzymes, α-amylase and α-glucosidase. A dose-dependent increase in the percentage of inhibitory activity of APE against α-amylase and α-glucosidase was observed. The calculated IC_{50} values of APE for the α-amylase and α-glucosidase assays were 54.26 ± 0.14 and 26.47 ± 0.12 μg/ml, respectively. In contrast, those of acarbose were 54.08 μg/ml and 61.93 μg/ml for α-amylase and α-glucosidase, respectively (Fig. 5).

3.5.2. Cytotoxicity assay

The cytotoxicity of APE against the 3T3L1 cell line was studied. The

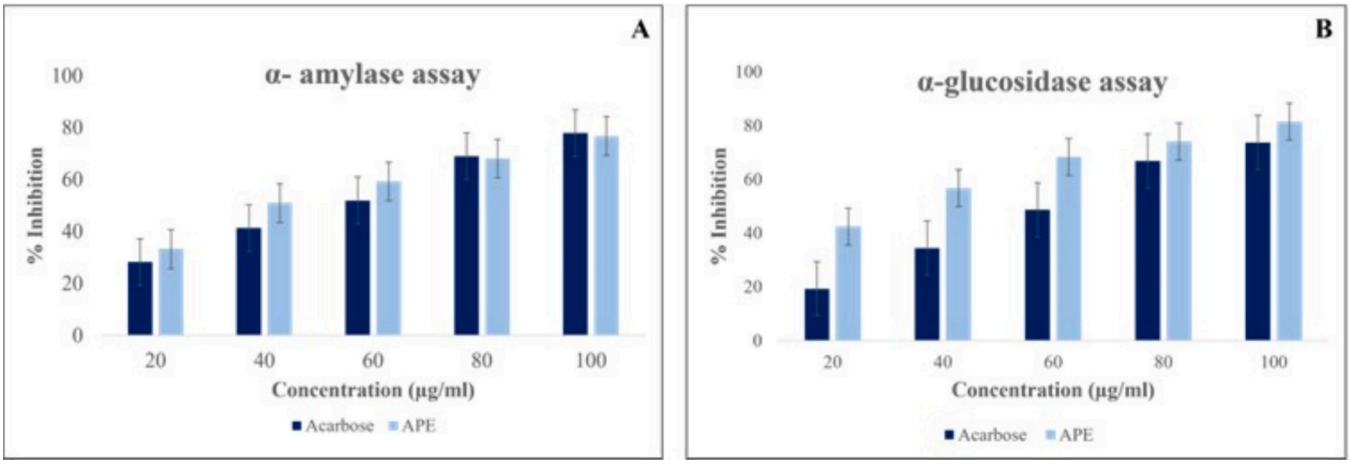

Fig. 5. A. α-amylase assay of acarbose and APE. **B.** α-Glucosidase assay of acarbose and APE. Promising inhibitory activity of APE against both enzymes, α-amylase and α-glucosidase, was observed compared with that of acarbose.

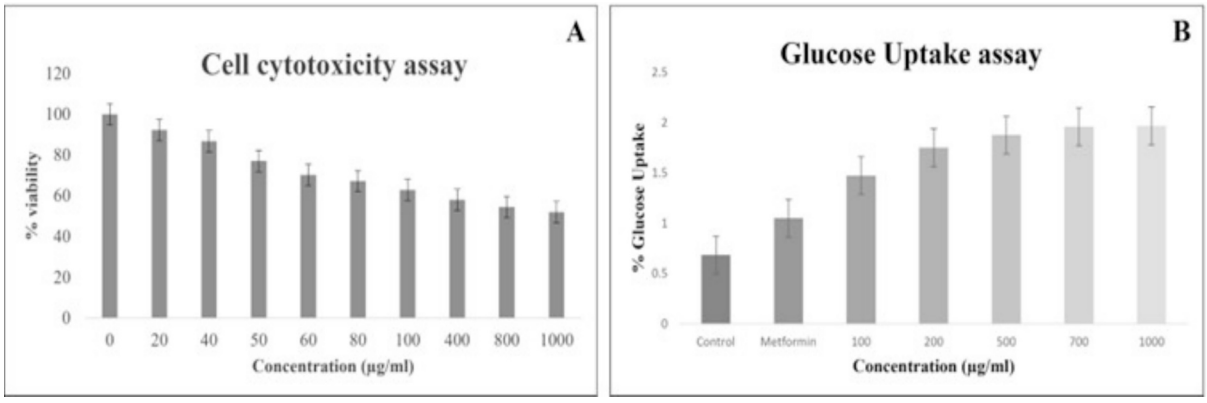

Fig. 6. A. Cell viability assay of the APE extract. **B.** Glucose uptake assay of starved MIN6 cells treated with increasing concentrations of APE. The percentage of glucose uptake by the cells was dose dependent with APE treatment.

Table 5
Physiochemical parameters of the APE-treated animals and normal control animals.

Body weight (in gm)		
Days	Normal	Treated
1	191.06 ± 3.21	202.1 ± 14.09
7	194.2 ± 4.57	208.1 ± 10.27
14	199.01 ± 8.87	213.5 ± 6.24
21	203.1 ± 4.26	215 ± 13.17
28	206.4 ± 4.4	217.1 ± 12.67
Food intake (in gm)		
1	13.76 ± 1.56	17.03 ± 2.03
7	13.82 ± 1.90	17.09 ± 1.62
14	16.24 ± 2.33	16.09 ± 2.32
21	15.21 ± 1.69	14.05 ± 1.03
28	14.63 ± 1.69	15.76 ± 2.51
Water intake (in ml)		
1	16.78 ± 2.54	18.1 ± 2.08
7	20.52 ± 1.97	19.34 ± 2.14
14	20.71 ± 1.95	21.34 ± 2.15
21	22.15 ± 1.16	23.42 ± 1.78
28	24.21 ± 3.12	23.91 ± 3.14

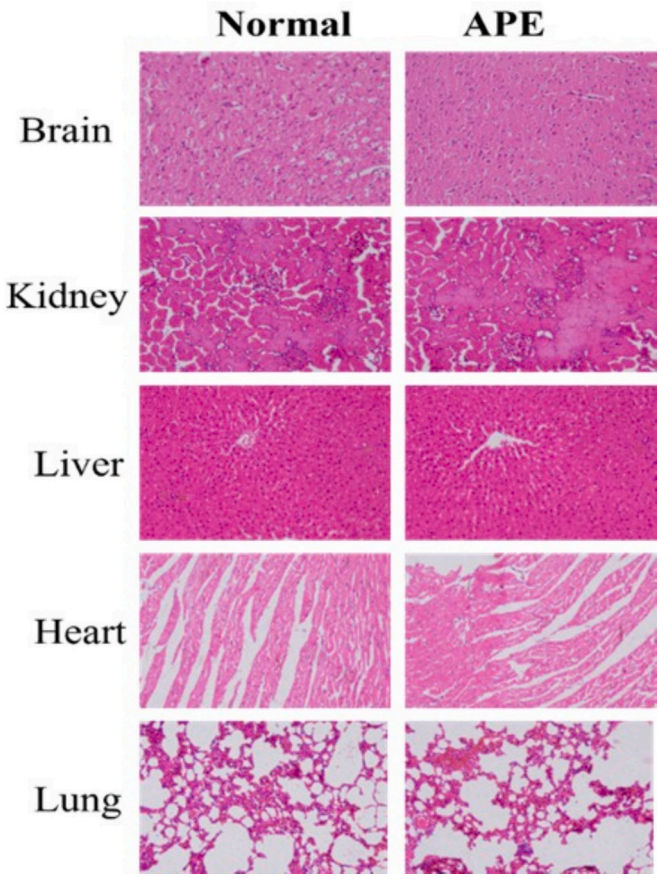

Fig. 7. H&E staining of vital organs from the toxicity study revealed no observable pathological alterations.

variable concentrations of APE and the percentage of viable cells were plotted (Fig. 6 A). Notably, even at a relatively high concentration of APE, the cell viability was 56.10 % after 48 h of exposure, and the calculated IC_{50} value was 1025 ± 3.011 μg/ml. These findings suggest that APE can be utilized for further *in vitro* antidiabetic studies without compromising cell viability.

3.5.3. Glucose uptake assay

Glucose-starved MIN6 cells treated with lower concentrations of glucose presented 30% glucose uptake. In contrast, the cells treated with higher concentrations of APE presented 80% glucose uptake compared with the control (Fig. 6 B). The percentage of glucose uptake by starved MIN6 cells treated with APE suggested a dose-dependent increase. Higher glucose uptake indicates insulin mimic activity, improved glucose homeostasis, and upregulation of the GLT4 transporter, which leads to increased insulin secretion with APE treatment.

3.6. In vivo antidiabetic study

3.6.1. Acute toxicity effect of APE

In the oral acute toxicity study, the animals in groups I-V did not exhibit any mortality at different doses. The effective dose of APE was calculated as 500 mg/kg body weight and was administered to diabetic experimental animals.

3.6.2. Subacute effects of APE

A subacute toxicity study of APE in animals revealed no symptoms of mortality or clinical changes throughout the experiment. The body weight, food, and water intake (Table 4), haematological (Table 5 A), and biochemical parameters (Table 5 B) did not significantly differ from those of the normal group.

H&E staining of the organs revealed no pathological alterations. The brain tissue exhibited intact neuronal structures without any inflammation or necrosis. The kidney tissue displayed normal glomerular and tubular architecture, confirming that there was no nephrotoxicity. Liver tissue showed normal architecture of hepatic cells with no hepatocellular damage. Heart tissue appeared normal, without signs of myocardial injury or inflammation. The lung tissue exhibited healthy alveolar structures that were free from inflammation, fibrosis, or cellular necrosis (Fig. 7).

3.6.3. Effect of APE on body weight, blood glucose level and HbA1c level

The physical and biochemical parameters, such as body weight, blood glucose level, and HbA1c level, of the experimental animals were measured, and the results were compared at the end of the experiment on the 28th day (Table 6). The normal group had a body weight of 243 ± 2.01 g; however, the body weight of the diabetes group was reduced significantly ($p < 0.001$) to 97 ± 1.98 g. In contrast, the body weights of the metformin-treated (132 ± 3.04 g) and APE-treated (290 ± 2.21 g) groups were significantly improved. The blood glucose level was significantly ($p < 0.001$) greater (467 ± 3.00 mg/dl) in the diabetic group than in the normal group (109 ± 1.56 mg/dl). However, the APE-treated group was reduced significantly ($p < 0.001$) to 130 ± 1.45 mg/dl, which was comparable with the metformin-treated group (110 ± 1.45 mg/dl). The HbA1c level was 5.13 ± 0.54 in the normal group, which significantly ($p < 0.001$) increased to 15.1 ± 0.02 in the diabetic group. However, upon the administration of APE, the HbA1c level was significantly ($p < 0.001$) reduced to 5.9 ± 0.01 and was comparable to that in the metformin-treated group (5.5 ± 0.05).

3.6.4. Effect of APE on serum marker levels

To determine the effect of APE on liver and kidney function, which is associated with long-standing diabetes, we measured the clinically proven serum markers LFT (alanine aminotransferase, aminotransferase, alkaline phosphatase) and KFT (urea and creatinine). In addition, several other parameters, such as cholesterol, total protein, triglycerides, high-density lipoprotein, and insulin, were measured in all the experimental groups. The diabetes group presented significantly elevated levels of serum markers such as insulin and ALB ($p < 0.001$), and the levels of other serum markers were significantly ($p < 0.001$) disturbed due to decreased insulin sensitivity and hyperglycemic conditions. In contrast, the APE- and metformin-treated groups were similar to the normal group (Table 7).

Table 6
Haematological and biochemical parameters of the APE-treated and control groups.

A. Haematological parameter				
	Normal	Diabetic	Metformin treated	APE treated
White blood cell count (WBC (10^3/l))	5.466 ± 0.249	14.8 ± 0.653	5.633 ± 0.169	7.466 ± 0.205
Neutrophils (Neu# (10^3/l))	4.466 ± 0.286	12.433 ± 0.235	5.5 ± 0.081	6.666 ± 0.262
Lymphocytes (Lym# (10^3/l))	3.466 ± 0.249	8.933 ± 0.368	2.633 ± 0.124	3.9 ± 0.163
Monocytes (Mon# (10^3/l))	0.433 ± 0.124	2.766 ± 0.286	0.3 ± 0.081	0.6 ± 0.081
Eosinophils (Eos# (10^3/l))	0.123 ± 0.028	0.8 ± 0.081	0.033 ± 0.012	0.026 ± 0.004
Basophil (bas# (10^3/l))	0.05 ± 0.024	0.633 ± 0.124	0.03 ± 0.008	0.06 ± 0.016
NLR	1.466 ± 0.169	7.233 ± 0.41	1.5 ± 0.081	2.4 ± 0.326
PLR	0.019 ± 0.001	0.06 ± 0	0.072 ± 0.076	0.025 ± 0.002
Red blood cell count (RBC (10^12/l))	5.866 ± 0.286	9.4 ± 0.163	5.3 ± 0.163	5.9 ± 0.163
Hemoglobin (HGB (g/dL))	13.5 ± 0.294	20.533 ± 0.205	13.4 ± 0.216	14.166 ± 0.368
HCT	43.633 ± 0.169	59.433 ± 0.169	43.566 ± 0.124	46.766 ± 1.228
MCV (fL)	84.433 ± 0.124	98.666 ± 0.205	85.5 ± 0.141	87.066 ± 1.755
MCH (pg)	30.133 ± 0.249	44.566 ± 0.286	30.433 ± 0.205	30.866 ± 0.612
MCHC (g/l)	327 ± 1.632	392.333 ± 2.054	336 ± 1.632	344.333 ± 11.841
RDW-CV	12.7 ± 0.326	20.633 ± 0.124	13.333 ± 0.205	14.066 ± 0.385
RDW-SD (fL)	37.5 ± 0.244	65.533 ± 0.249	40.466 ± 0.169	45.333 ± 3.633
Platelet count (PLT (10^3/l))	2.733 ± 0.124	6.7 ± 0.216	3.366 ± 0.124	5 ± 0.216
MPV (fL)	10.5 ± 0.244	18.533 ± 0.205	11.266 ± 0.124	11.866 ± 0.169
PDW-CV	50.6 ± 0.163	78.533 ± 0.286	53.333 ± 0.205	67.1 ± 0.668
PDW-SD (fL)	10.566 ± 0.205	20.6 ± 0.244	14.433 ± 0.205	14.933 ± 0.449
PCT (ml/l)	0.164 ± 0.003	0.544 ± 0.002	0.125 ± 0.001	0.223 ± 0.039

B. Biochemical parameter					
Parameter	**Normal**	**Diabetic**	**Metformin treated**	**APE treated**	**Ref range**
Glucose (GLU) mg/dl	116.51 ± 5.73	207.53 ± 58.89	90.98 ± 10.36	50.43 ± 5.97	74.0–143.0
Albumin (ALB) g/dl	2.95 ± 0.90	6.816 ± 0.59	2.2 ± 0.36	3.2 ± 0.50	2.3–4.0
Urea mg/dl	29.28 ± 6.31	14.876 ± 2.25	23.11 ± 3.36	33.81 ± 13.22	15.0–58.0
Creatinine (CREA) mg/dl	1.375 ± 0.48	25.15 ± 9.09	1.638 ± 0.17	1.63 ± 0.16	0.5–1.8
Cholesterol (CHOL) mg/dl	157.86 ± 28.42	28.51 ± 11.09	146.1 ± 13.74	169.9 ± 13.53	109.0–202.0
Triglycerides (TG) mg/dl	90.53 ± 45.79	191.44 ± 15.17	96.1 ± 33.69	123.25 ± 6.71	40.0–165.0
Alanine transaminase (ALT) U/l	84.53 ± 18.40	168.48 ± 13.89	84.53 ± 18.40	54.28 ± 1.94	10.00–125.00
Aspartate aminotransferase (AST) U/l	32.49 ± 4.40	121.76 ± 0.94	33.6 ± 3.68	20.4 ± 0.18	0–50.0
Total protein (TP) g/dl	5.548 ± 0.62	1.02 ± 0.85	6.14 ± 1.35	5.58 ± 0.65	5.2–8.2
Magnesium (MG) mg/dl	1.7 ± 0.16	0.316 ± 0.17	1.9 ± 0.35	1.86 ± 0.39	1.50–2.10
Phosphorus (PHOS) mg/dl	4.85 ± 0.75	33.22 ± 8.38	5.85 ± 1.36	5.383 ± 1.11	3.00–6.20
Calcium (CA) mg/dl	9.03 ± 0.36	64.21 ± 13.81	9.033 ± 0.78	9 ± 0.69	8.70–11.80
Direct bilirubin (DBIL) mg/dl	0.32 ± 0.17	6.2 ± 1.67	0.3803 ± 0.22	0.416 ± 0.15	0–0.50
Total bilirubin (TBIL) mg/dl	0.513 ± 0.29	10.93 ± 0.43	0.61 ± 0.32	0.52 ± 0.16	0–0.90
High-density lipoprotein (HDL) mg/dl	55.0166 ± 11.18	428.91 ± 33.72	54.88 ± 10.14	124.6 ± 1.90	35.0–88.0
Gamma-glutamyl transferase (GGT) U/l	5.13 ± 2.08	18.8 ± 7.09	6.083 ± 2.06	7.0286 ± 0.01	0–10.0
Alkaline phosphatase (ALP) U/l	122.46 ± 2.68	252.68 ± 21.60	75.23 ± 20.88	91.9 ± 12.52	0.1–212.0

3.6.5. Histopathological and immunohistochemical studies

H&E staining of the pancreatic islets revealed significant structural alterations in the diabetic group compared with the normal group. However, the APE-treated group presented a similar structure to that of the normal group (Fig. 8 A-D).

Immunohistochemistry (IHC) of the normal pancreas revealed strong staining for anti-synaptophysin (Fig. 8 AS), anti-insulin (Fig. 8 AI), and anti-glucagon (Fig. 8 AG) antibodies, indicating that intact synaptic function and robust insulin production subsequently maintain proper glucose homeostasis. In contrast, the diabetic pancreas presented a reduced intensity of synaptophysin-positive (synaptic) cells (Fig. 8 BS), whereas the insulin-stained pancreas was negative because of the destruction of β-cells (Fig. 8 BI). The proportion of glucagon-positive cells (α-cells) was greater (46 \%) than that in normal individuals [37] (Fig. 8 BG). This significant pathophysiological alteration was due to hyperglycemic conditions (including impaired insulin secretion). In the metformin-treated group, the number of anti-synaptophysin-stained slides was slightly greater than that in the diabetic group (Fig. 8 CS), but the expression of anti-insulin-stained slides was similar to that in the diabetic group (Fig. 8 CI), suggesting that metformin treatment partially restored synaptic function without modulating β-cells. The proportion of α-cells in the anti-glucagon-stained slides was similar to that in the diabetic group (Fig. 8 CG). In the APE-treated group, the pancreatic islets stained with an anti-synaptophysin antibody exhibited a significant increase in intensity, suggesting substantial restoration of synaptic function (Fig. 8 DS). The anti-insulin-stained slides showed restoration of β-cells. The calculated proportion of β-cells after four weeks of treatment was calculaterd to be 47% (Fig. 8 DI, Table 8). However, the anti-glucagon antibody-stained slides revealed the normal architecture of the α-cells (reduced proportion of α-cells) (Fig. 8 DG).

3.6.6. Analysis of immunohistochemical images

IHC images of all four groups of pancreata were taken using a microscope in the bright field region (Nikon Eclipse TS2R, Japan). The area proportions of the captured images were analysed via ImageJ software. Synaptophysin-stained slides were used to calculate the total area of the islet, insulin-stained slides were used to calculate the proportion of β-cells, and glucagon-stained slides were used to calculate the proportion of α-cells. The β-cell proportion was calculated to be 64% in the normal group, whereas 39.80% and 47% regeneration were calculated in the APE-treated group after the 21st and 28th days of treatment, respectively. In contrast, the glucagon proportion in the normal islets was 17%, whereas in diabetic islets, it was increased to 46%. However, in the APE-treated groups (21%), the proportion was similar to that in the normal group.

Table 7
Comparative study of body weight, blood glucose levels, and glycated hemoglobin (HbA1c) levels in different experimental groups on the 7th, 14th, 21st, and 28th days.

Body weight (g)				
	Day 7	Day 14	Day 21	Day 28
Normal	211 ± 1.6	224 ± 1.89	231 ± 0.98	243 ± 2.01
Diabetic	192 ± 3.45	122 ± 2.51	103 ± 3.12	97 ± 1.98 ***
Metformin treated	160 ± 3.01	140 ± 2.45	130 ± 1.67	132 ± 3.04 **
APE treated	222 ± 4.23	258 ± 2.78	278 ± 1.2	290 ± 2.21 ***
Blood glucose level (mg/dl)				
Normal	95 ± 2.06	88 ± 1.6	104 ± 3.00	109 ± 1.56
Diabetic	410 ± 4.72	459 ± 4.35	431 ± 1.00	467 ± 3.00 ***
Metformin treated	497 ± 2.59	330 ± 2.76	144 ± 1.12	110 ± 1.45 ***
APE treated	510 ± 1.52	367 ± 2.00	200 ± 2.00	130 ± 1.45 ***
Glycated hemoglobin (HbA1C) level (mmol/Mol)				
Normal	5.69 ± 0.8	4.89 ± 0.01	5.00 ± 0.56	5.13 ± 0.54
Diabetic	15.69 ± 0.20	14.8 ± 0.07	15.9 ± 0.07	15.1 ± 0.02 ***
Metformin treated	13.7 ± 0.01	9.3 ± 0.3	6.4 ± 0.05	5.56 ± 0.5 ***
APE treated	12.8 ± 0.08	10.7 ± 0.05	8.8 ± 0.2	6.5 ± 0.01 **

Statistical analysis was carried out via one-way ANOVA followed by the Tukey–Kramer multiple comparisons test. The values are presented as the means ± SEMs (n = 6). p < 0.05, p** < 0.01, p*** < 0.001, and * represent significant differences from the control.

4. Discussion

Dysfunction and apoptosis of pancreatic β-cells lead to the development of chronic metabolic illness diabetes. Diabetogenic agents such as streptozotocin and alloxan selectively destroy pancreatic β-cells via the induction of free radicals such as reactive oxygen species (ROS) and oxidative stress, subsequently resulting in impaired insulin secretion [36,38]. The key mechanism of alloxan and its metabolic product, dialuric acid, initiates a redox cycle to form a superoxide radical that destroys pancreatic β-cells [39–41]. The increasing prevalence of diabetes poses a significant health concern globally [42]. Despite the availability of antidiabetics, these drugs have adverse side effects, including urinary dysfunction and elevated lipid profiles, during long-term use [43].

The current study focused mainly on developing a polyherbal formulation with antihyperglycemic effects and reviving destroyed pancreatic β-cells. APE was prepared by mixing sixteen medicinal plants known for their antidiabetic activity on the basis of traditional methods. An analytical study of APE revealed the presence of several bioactive compounds with antidiabetic activity. The *in-silico* study revealed that verbacoside B has good binding affinity for the IGF-I and GLUT4 proteins, suggesting that this compound can improve insulin secretion and inhibit carbohydrate digestive enzymes. An in vitro study using the MIN6 cell line revealed increased glucose uptake in APE-treated cells, suggesting increased insulin secretion for the maintenance of blood glucose levels. These results suggest increased glucose uptake in a dose-dependent manner, suggesting that the insulin-mimetic activity of APE improved glucose homeostasis and upregulated the GLUT4 transporter to regulate blood glucose levels. The same result was reported in a previous study on pancreatic β-cell lines (MIN6 and cultured islets), suggesting that flavonoids can increase insulin secretion, inhibit cell apoptosis, and promote the proliferation of pancreatic β-cells [44].

The contemporary results for blood glucose and HbA1c levels were in line with those of a previous report that APE significantly decreases blood glucose and hemoglobin (HbA1C) levels among alloxan-induced diabetic animals [41,45]. This may be due to the extrapancreatic action of APE, which results in a significant decrease in the blood glucose level. The increasing body weights of the treatment group indicate the ability of APE to reverse the hyperglycemic effects of the chemical or its treasured phytoconstituents [41]. The adverse effects of diabetes related to HbA1c are associated primarily with protein glycosylation, which leads to many other complications, including vascular, nerve, and kidney damage; eye complications; and impaired wound healing [46]. Plants such as *Cinnamomum cassia, Catharanthus roseus,* and *Gymnema sylvestre* decrease the HbA1c level during treatment [47–49]; the same finding was reported in the present study. This may be due to the presence of phytochemicals such as tannins, sterols, phenolic acids, and phenolic compounds, which are responsible for the antidiabetic properties [50]. In addition, an analytical study revealed the presence of neocaesalpin c, luteolin-5-o-glucoside, tannic acid, isovitexin 6″-o-glucoside, gallic acid, mangiferin, noreugenin, litseglutine b, apigenin 7-apiosyl-glucoside, 14-deoxy-11,12-didehydroandrographiside, azadirachtin I, and δ-caesalpin in the extract, which reportedly decrease the blood glucose level by increasing the rate of glucose absorption by the intestine, reducing hepatic glucose production, increasing insulin sensitivity, reducing oxidative stress and inflammation in the body, and inhibiting carbohydrate metabolism enzymes [44,51–58].

In diabetes, kidney functions are affected, leading to glomerular hyperfiltration and microalbuminuria via increased urea and creatinine levels [45,59]. The present study demonstrated that the diabetic group presented elevated serum levels of different markers compared with those in the normal group. In contrast, the results of the metformin- and APE-treated groups were similar to those of the normal group. The current findings on the serum levels were consistent with the results reported previously [60].

Recent studies have revealed that endogenous pancreatic β-cell regeneration may mitigate diabetes symptoms. The results of the present study aligned with those reported earlier [60], i.e., immunostaining revealed a restoration of the pancreatic β-cells with APE treatment in diabetic models and indicated the normal mantle core architecture of the islet. The results of the present study suggest an increase in insulin secretion with APE treatment. Moreover, ongoing clinical trials are evaluating the safety and efficacy of medicinal plant-based interventions, further contributing to the evidence supporting their use in diabetes care. This research seeks to validate traditional knowledge and potentially integrate these natural remedies into conventional medical practices.

A literature review revealed that medicinal plants regenerate pancreatic β-cells via regeneration from non β-cells or stem/progenitor cells and through increased proliferation of preexisting β-cells [10]. Plants such as *Agaricus bisporus* [61], *Aralia taibaiensis* via the Wnt, β-catenin, and TCF7L2 pathways [62], *Ervatamia microphylla* [63], *Glycine* max via the cAMP/PKA signalling pathway [64], *Rhodiola rosea* by activating Akt/FoxO1 signalling [65], *Mangifera indica* via STAT3 signalling [66], and *Tinospora cordifolia* by increasing the expression of Pdx-1 mRNA and decreasing the expression of carbonic anhydrase nine mRNAs, *Radix puerariae* via the GLP-1R, Wnt, and STAT signalling pathways [67], have been reported to regenerate β-cells. The plants capable of increasing β-cell mass through proliferation include *Angelica sinensis, Hibiscus rosa-sinensis, Woodfordia fruticosa, Cornus officinalis, salidroside,* and *sangguayin* [68]. The above mechanistic study revealed that natural bioactive compounds are responsible for β-cell regeneration and the improvement of β-cell function. The compounds identified from APE, such as apigenin 7-apiosyl-glucoside, arjunolic acid, verbascoside B, arjungenin, gymnemic acid I, ii, iv, xiii, and ricinoleic acid, are responsible for the regeneration and proliferation of β-cells, as reported previously [54,69–73].

The regeneration of pancreatic β-cells can be assessed through histopathological examination of pancreatic tissue, alongside immunohistochemical (IHC) analysis for both semiquantitative and quantitative measurements of insulin-positive cells and proliferating β-cells [74]. The present study demonstrated the regeneration of pancreatic β-cells in alloxan-induced animals treated with APE, and the calculated percentage of β-cell regeneration was 47 %. This study suggested that the

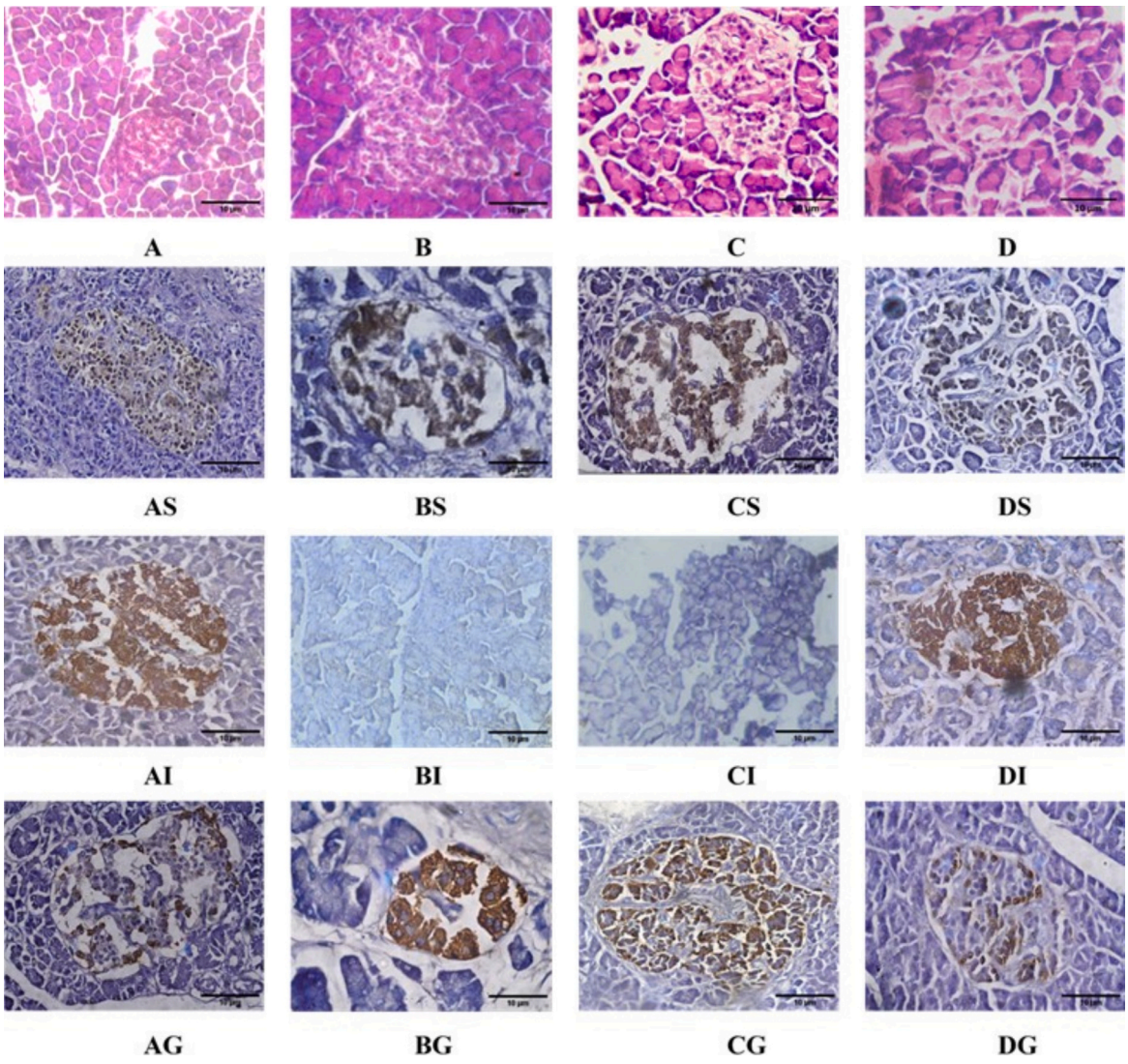

Fig. 8. Histopathological and immunohistological images of the pancreas in experimental animals. **A-D.** H&E staining of pancreatic islets from the normal, diabetic, metformin-treated, and APE-treated groups. IHC staining of the pancreatic islets with an anti-synaptophysin antibody (**AS-DS**), anti-insulin antibody (**AI-DI**) and anti-glucagon antibody (**AG-DG**).

regeneration of β-cells may be due to the presence of bioactive compounds such as polyphenols, tannins, and flavonoids. Phytochemical analysis revealed a rich source of secondary metabolites, such as alkaloids, terpenoids, saponins, glycosides, flavonoids, tannins, and steroids [75]. Additionally, an in silico study revealed the strong binding affinity of verbascoside B (identified from APE) with the insulin-like growth factor I (IGF—I) protein, suggesting a potential role in enhancing insulin secretion. This interaction could modulate the IGF-I signalling pathway, which is known to influence pancreatic β-cell function and glucose homeostasis, thereby offering promising therapeutic benefits for managing diabetes. In addition to these other phytoconstituents, the ability of mangiferin identified from APE to regenerate and enhance β-cell function in animal models has been well studied [43,76].

5. Conclusion

The current findings confirm that APE has prominent antidiabetic activity, as evidenced by *in silico*, *in vitro,* and *in vivo* studies, by modulating the cellular composition and regenerating pancreatic β-cells, leading to sufficient insulin secretion. An *in silico* study revealed that by modulating the IGF-I signalling pathway, this bioactive compound enhanced insulin secretion and pancreatic β-cell functions. The *in vitro* study revealed substantial inhibition of carbohydrate digestive enzymes and improved cellular glucose uptake with treatment. Significant restoration of biochemical serum markers and regeneration of pancreatic β-cells were observed in the APE treated group. More studies are needed to elucidate the exact mechanism of action. APE can be used as an active ingredient for developing various solid oral dosage forms subjected to its stability with different excipients. In addition, our team has commenced studies at the molecular level to determine the primary mechanism and elucidate the method of action by which APE targets a particular gene that is responsible for diabetes.

CRediT authorship contribution statement

Abhijit Sahu: Writing – original draft, Software, Methodology, Formal analysis, Data curation, Conceptualization. **Pravash Ranjan Mishra:** Writing – review & editing, Supervision, Resources, Project administration, Funding acquisition, Conceptualization. **Pratyush Pragyandipta:** Methodology, Formal analysis. **Srichandan Rath:** Methodology, Formal analysis. **Ashirbad Nanda:** Methodology. **Satish Kanhar:** Writing – review & editing, Methodology, Formal analysis. **Dibya Ranjan Sahoo:** Methodology. **Eeshara Naik:** Methodology. **Deepali Naik:** Methodology. **Pradeep K. Naik:** Writing – review &

Table 8
Biochemical estimation of different serum markers in experimental animals.

Biochemical Test	Normal	Diabetic	Metformin Treated	APE Treated
Kidney function test (KFT)				
UREA (mg/dl)	49.686 ± 3.227	66.35 ± 1.75***	46.73 ± 3.97***	44.43 ± 0.25***
CREA (mg/dl)	1.316 ± 0.157	26.42 ± 1.74***	1.5 ± 0.26***	1.41 ± 1.4***
Liver function test/liver enzyme (LFT)				
SGPT (U/l)	100.76 ± 5.24	154.95 ± 2.90***	115.666 ± 3.85***	122.08 ± 3.3***
SGOT (U/l)	32.316 ± 2.070	324.3 ± 4.57***	43.85 ± 1.31***	43 ± 1.7***
ALB (g/dl)	2.523 ± 0.155	0.81 ± 0.487***	2.631 ± 0.16***	3.156 ± 0.6***
ALP (U/l)	41.016 ± 4.460	254.45 ± 10.91***	48.25 ± 2.88***	54 ± 1.2***
Other biochemical parameter				
CHOL (mg/dl)	116.666 ± 3.85	7.316 ± 4.09***	108.33 ± 3.19***	98 ± 12.4***
TG (mg/dl)	126.316 ± 2.4	229.88 ± 9.40***	133.2 ± 2.93***	151.40 ± 38.2***
TP (g/dl)	5.583 ± 1.129	2.81 ± 0.55***	4.691 ± 0.33***	4.1 ± 10.3***
HDL (mg/dl)	69.568 ± 5.201	12.43 ± 55.4***	70.7 ± 5.66***	84.38 ± 5.4***
Insulin (μU/ml)	2.01 ± 0.01	0.015 ± 0.005***	1.3 ± 0.015***	2.15 ± 0.7***

editing, Supervision, Resources, Project administration, Funding acquisition, Conceptualization.

Declaration of competing interest

The authors declare that they have no known competing financial interests or personal relationships that could have appeared to influence the work reported in this paper.

Acknowledgements

This work has received support from the DBT BUILDER, Govt. of India, Department of Biotechnology and Bioinformatics, Sambalpur University, Grant no: BT/INF/22/SP45357/2022. The laboratory support of the Centre of Excellence in Natural Products and Therapeutics (COE-NPT) is highly acknowledged for the smooth execution of the research work.

Data availability

Data will be made available on request.

References

[1] R.M. Anjana, R. Unnikrishnan, M. Deepa, R. Pradeepa, N. Tandon, A.K. Das, S. Joshi, S. Bajaj, P.K. Jabbar, H.K. Das, A. Kumar, V.K. Dhandhania, A. Bhansali, P. V. Rao, A. Desai, S. Kalra, A. Gupta, R. Lakshmy, S.V. Madhu, N. Elangovan, S. Chowdhury, U. Venkatesan, R. Subashini, T. Kaur, R.S. Dhaliwal, V. Mohan, V. Sudha, E. Nirmal, L.M. Nath, J. Mahanta, A. Pandey, M.N. Rao, L. Jampa, T. Kaki, P.K. Borah, S. Sharma, K. Dash, V.K. Shrivas, A. Krishnan, A. Dias, B. Saboo, J.M. Padhiyar, B. Kalra, J.K. Mokta, R. Gulepa, P. Adhikari, S. Rao, C. Jayakumari, S.M. Jain, G. Gupta, C.S. Yajnik, P.P. Joshi, S. Ningombam, T. B. Singh, R.O. Budnah, M.R. Basaiawmoit, P.C. Rosangluaia, V. Lalramenga, S. Suokhrie, S.K. Tunyi, N.C. Tripathy, A.J. Sahu, M. Purty, B.L. John, S.K. Gupta, K.J. Shrivastava, T.T. Tobgay, T. Kaleon, S.K. Reang, M.K. Das, S. Mathur, R. Modi, S. Ghosh Kakkar, Metabolic non-communicable disease health report of India: the ICMR-INDIAB national cross-sectional study (ICMR-INDIAB-17), Lancet Diabetes Endocrinol. 11 (2023) 474–489, https://doi.org/10.1016/S2213-8587(23)00119-5.

[2] W. Cabrera, S. Genta, A. Said, A. Farag, K. Rashed, S. Sánchez, Hypoglycemic activity of *Ailanthus excelsa* leaves in normal and streptozotocin-induced diabetic rats, Phytother. Res. 22 (2008) 303–307, https://doi.org/10.1002/ptr.2311.

[3] D.J. Steiner, A. Kim, K. Miller, M. Hara, Pancreatic islet plasticity: interspecies comparison of islet architecture and composition, Islets 2 (2010), https://doi.org/10.4161/ISL.2.3.11815.

[4] D. Bosco, M. Armanet, P. Morel, N. Niclauss, A. Sgroi, Y.D. Muller, L. Giovannoni, G. Parnaud, T. Berney, Unique arrangement of alpha- and beta-cells in human islets of Langerhans, Diabetes 59 (2010) 1202–1210, https://doi.org/10.2337/DB09-1177.

[5] H.H. Huang, S. Harrington, L. Stehno-Bittel, The flaws and future of islet volume measurements, Cell Transplant. 27 (2018) 1017–1026, https://doi.org/10.1177/0963689718779898.

[6] P. Mishra, A. Sahu, P.K. Naik, P.K. Ravi, Islet dimensions and its impact on the cellular composition and insulin-secreting capacity: insights into the role of non-beta cells, Cureus (2024), https://doi.org/10.7759/cureus.52428.

[7] G. Kilimnik, J. Jo, V. Periwal, M.C. Zielinski, M. Hara, Quantification of islet size and architecture, Islets 4 (2012) 167–172, https://doi.org/10.4161/isl.19256.

[8] O.M. Ighodaro, A.M. Adeosun, O.A. Akinloye, Alloxan-induced diabetes, a common model for evaluating the glycemic-control potential of therapeutic compounds and plants extracts in experimental studies, Medicina (B Aires) 53 (2017) 365–374, https://doi.org/10.1016/j.medici.2018.02.001.

[9] E. Susilawati, J. Levita, Y. Susilawati, S.A. Sumiwi, Review of the Case Reports on Metformin, Sulfonylurea, and Thiazolidinedione Therapies in Type 2 Diabetes Mellitus Patients, Medical Sciences (2023), https://doi.org/10.3390/MEDSCI11030050. Vol. 11, Page 50 11 (2023) 50.

[10] C.N. Kimani, H. Reuter, S.H. Kotzé, C.J.F. Muller, Regeneration of pancreatic Beta cells by modulation of molecular targets using plant-derived compounds: pharmacological mechanisms and clinical potential, Curr. Issues Mol. Biol. 45 (2023) 6216–6245, https://doi.org/10.3390/cimb45080392.

[11] F. Zhong, Y. Jiang, Endogenous pancreatic β cell regeneration: a potential strategy for the recovery of β cell deficiency in diabetes, Front Endocrinol (Lausanne) 10 (2019) 101, https://doi.org/10.3389/FENDO.2019.00101.

[12] S. Paul, M. Majumdar, Exploring antidiabetic potential of a polyherbal formulation Madhurakshak Activ: an in vitro and in silico study, Fitoterapia 169 (2023), https://doi.org/10.1016/J.FITOTE.2023.105598.

[13] M.T. Akhtar, T. Almas, S. Safdar, M. Saadia, R. Qadir, S. Batool, M. Mustaqeem, U. Ali Shaukat, F. Kanwal, R. Cai, Antioxidant, Hypoglycemic, Antilipidemic, and Protective Effect of Polyherbal Emulsion (F6-SMONSECCE) on Alloxan-Induced Diabetic Rats, ACS Omega 8 (2023) 21642–21652, https://doi.org/10.1021/ACSOMEGA.3C01027.

[14] G. Revathi, S. Elavarasi, K. Saravanan, B. Bahadur, Traditional Use of Herbal Plants for the Treatment of Diabetes in India. https://www.researchgate.net/publication/315738809, 2016.

[15] J. Das, B.C. Acharya, S.N. Mallick, Traditional ethno-medicinal plants used for treatment of diabetes by Bhuyan tribes in Sundargarh District of Odisha, India-An Ethnobotanical Survey, Plant Science Today 10 (2023) 58–67, https://doi.org/10.14719/pst.2030.

[16] M.R. Rafe, A review of five traditionally used anti-diabetic plants of Bangladesh and their pharmacological activities, Asian Pac, J. Trop. Med. 10 (2017) 933–939, https://doi.org/10.1016/j.apjtm.2017.09.002.

[17] T. Thirumalai, B.C. David, K. Sathiyaraj, B. Senthilkumar, E. David, Ethnobotanical study of anti-diabetic medicinal plants used by the local people in Javadhu hills Tamilnadu, India, Asian Pac. J. Trop. Biomed. 2 (2) (2012) S910–S913. www.elsevier.com/locate/apjtb.

[18] M. Jyoti, A. Kshitij, S. Vivek, S. Prem, Preparation and standardization of a Polyherbal formulation, J Adv Sci Res 3 (2012) 84–85. https://sciensage.info/index.php/JASR/article/view/104.

[19] A. Sherikar, M. Mahanthesh, Evaluation of aqueous and methanolic extract of leaves of Epipremnum aureum for radical scavenging activity by DPPH method, total phenolic content, reducing capacity assay and FRAP assay, J Pharmacogn Phytochem 4 (2015) 36–40. https://www.phytojournal.com/archives/2015.v4.i4.678/evaluation-of-aqueous-and-methanolic-extract-of-leaves-of-epipremnum-aureum-for-radical-scavenging-activity-by-dpph-method-total-phenolic-content-reducing-capacity-assay-and-frap-assay.

[20] A.M. Salih, F. Al-Qurainy, M. Nadeem, M. Tarroum, S. Khan, H.O. Shaikhaldein, A. Al-Hashimi, A. Alfagham, J. Alkahtani, Optimization Method for Phenolic Compounds Extraction from Medicinal Plant (Juniperus procera) and Phytochemicals Screening, Molecules 26 (7454) (2021) 26, https://doi.org/10.3390/MOLECULES26247454.

[21] S. Baliyan, R. Mukherjee, A. Priyadarshini, A. Vibhuti, A. Gupta, R.P. Pandey, C.-M. Chang, Determination of antioxidants by DPPH radical scavenging activity and quantitative phytochemical analysis of Ficus religiosa, Molecules 27 (2022) 1326, https://doi.org/10.3390/molecules27041326.

[22] O.E. Adebiyi, F.O. Olayemi, T. Ning-Hua, Z. Guang-Zhi, *In vitro* antioxidant activity, total phenolic and flavonoid contents of ethanol extract of stem and leaf of Grewia carpinifolia, Beni Suef Univ J Basic Appl Sci 6 (2017) 10–14, https://doi.org/10.1016/j.bjbas.2016.12.003.

[23] M. Naik, S. Behera, S. Induar, S.K. Babu, P.K. Naik, Elemental, nutritional, and phytochemical profiling and antioxidant activity of Cordia obliqua Willd. (clammy cherry): an important underutilized forest tree of East India, J Appl Biol Biotechnol 11 (2023) 195–199, https://doi.org/10.7324/JABB.2023.110127.

[24] P. Pragyandipta, R.K. Pedapati, P.K. Reddy, A. Nayek, R.K. Meher, S.K. Guru, S. Kantevari, P.K. Naik, Rational design of novel microtubule targeting anticancer drugs N-imidazopyridine noscapinoids: chemical synthesis and experimental evaluation based on *in vitro* using breast cancer cells and *in vivo* using xenograft mice model, Chem. Biol. Interact. 382 (2023), https://doi.org/10.1016/J.CBI.2023.110606.

[25] L. Vo Van, E.C. Pham, C.V. Nguyen, N.T.N. Duong, T. Vi Le Thi, T.N., Truong, *in vitro* and *in vivo* antidiabetic activity, isolation of flavonoids, and *in silico* molecular docking of stem extract of Merremia tridentata (L.), Biomed. Pharmacother. 146 (2022) 112611, https://doi.org/10.1016/J.BIOPHA.2021.112611.
[26] P. Pragyandipta, M.R. Naik, B. Bastia, P.K. Naik, Development of 9-(N-arylmethylamino) congeners of noscapine: the microtubule targeting drugs for the management of breast cancer, 3 Biotech 13, 2023, https://doi.org/10.1007/S13205-022-03445-3.
[27] S. Rath, K. Kalimuthu, K. Naidu, R. Sivaramakrishnan, S. Rath, K. Kapilan, N. Kavitha, S. Kanchana, M. Arumugam, *In vitro* anti-diabetic and anti-inflammatory activities of metabolites isolated from Marine Sponge, *Heteronema erecta* (Keller, 1889) and it's *in silico* studies. https://www.researchgate.net/publication/346303743, 2020.
[28] S. Soeng, E. Evacuasiany, W. Widowati, N. Fauziah, V.T. Manik, M. Maesaroh, Inhibitory potential of rambutan seeds extract and fractions on adipogenesis in 3T3-L1 cell line, J Exp Integr Med 5 (2015) 55–60, https://doi.org/10.5455/JEIM.200115.OR.120.
[29] S. Dubey, D. Kumar, M.H. Wellness, A. Acharya, F. Cytometry, K. Mishra, S. Dubey, S. Bole, Study of glucose uptake activity of *aegle marmelos* ethanolic extract on liver cell line by flow cytometry study of glucose uptake activity of *aegle marmelos* ethanolic extract on liver cell line, Dubey et al. World Journal of Pharmacy and Pharmaceutical Sciences 7, 2018, https://doi.org/10.20959/wjpps20186-11796.
[30] M. Alsawalha, P. Janardhana, K. Padma, S. Reddy, A. Al-Subaie, S. Bolla, V. Veeraraghavan, J. Joseph, S. Mohan, S. Mohan, Study of antidiabetic properties of Uvaria narum leaf extract through glucose uptake and glucose transporter 4 expression studies in 3T3L1 cell line model, Pharm. Res. 11 (2019) 304, https://doi.org/10.4103/pr.pr_7_19.
[31] Test No. 407: Repeated Dose 28-day Oral Toxicity Study in Rodents, 2008, https://doi.org/10.1787/9789264070684-EN.
[32] S. Kanhar, A.K. Sahoo, Ameliorative effect of Homalium zeylanicum against carbon tetrachloride-induced oxidative stress and liver injury in rats, Biomed. Pharmacother. 111 (2019) 305–314, https://doi.org/10.1016/j.biopha.2018.12.045.
[33] T.B. Devi, S. Jena, B. Patra, K.D. Singh, S. Chawla, V. Raina, A.S. Koijam, A. Parida, Y. Rajashekar, Acute and sub-acute toxicity evaluation of dihydro-p-coumaric acid isolated from leaves of Tithonia diversifolia Hemsl, A. Gray in BALB/c mice, Front Pharmacol 13 (2022) 1055765, https://doi.org/10.3389/FPHAR.2022.1055765/BIBTEX.
[34] A. Hamadjida, R.E.A. Mbomo, S.E. Minko, F. Ntchapda, J.P. Kilekoung Mingoas, N. Nnanga, Antioxidant and anti-inflammatory effects of Boswellia dalzielii and Hibiscus sabdariffa extracts in alloxan-induced diabetic rats, Metabol Open 21 (2024) 100278, https://doi.org/10.1016/j.metop.2024.100278.
[35] A. Mollica, G. Zengin, M. Locatelli, A. Stefanucci, G. Macedonio, G. Bellagamba, O. Onaolapo, A. Onaolapo, F. Azeez, A. Ayileka, E. Novellino, An assessment of the nutraceutical potential of Juglans regia L. leaf powder in diabetic rats, Food Chem. Toxicol. 107 (2017) 554–564, https://doi.org/10.1016/J.FCT.2017.03.056.
[36] N.I. El-Desouki, G.A. Tabl, K.K. Abdel-Aziz, E.I. Salim, N. Nazeeh, Improvement in beta-islets of Langerhans in alloxan-induced diabetic rats by erythropoietin and spirulina, the journal of basic & applied, Zoology 71 (2015) 20–31, https://doi.org/10.1016/j.jobaz.2015.04.003.
[37] L.A.D. Queiroz, J.B. Assis, J.P.T. Guimarães, E.S.A. Sousa, A.C. Milhomem, K.K. S. Sunahara, A. Sá-Nunes, J.O. Martins, Endangered lymphocytes: the effects of Alloxan and Streptozotocin on immune cells in type 1 induced diabetes, Mediat. Inflamm. 2021 (2021) 1–15, https://doi.org/10.1155/2021/9940009.
[38] A. Taheriazam, M. Entezari, Z.M. Firouz, S. Hajimazdarany, M. Hossein Heydargoy, A.H. Amin Moghadassi, A. Moghadaci, A. Sadrani, M. Motahhary, A. Harif Nashtifani, A. Zabolian, T. Tabari, M. Hashemi, R. Raesi, M. Jiang, X. Zhang, S. Salimimoghadam, Y.N. Ertas, D. Sun, Eco-friendly chitosan-based nanostructures in diabetes mellitus therapy: promising bioplatforms with versatile therapeutic perspectives, Environ. Res. 228 (2023) 115912, https://doi.org/10.1016/J.ENVRES.2023.115912.
[39] T. Szkudelski, The mechanism of alloxan and streptozotocin action in B cells of the rat pancreas, Physiol. Res. 50 (2001) 537–546, https://pubmed.ncbi.nlm.nih.gov/11829314/(accessed April 4, 2024).
[40] W.H. El-Tantawy, E.N.A. Al Haleem, Therapeutic effects of stem cell on hyperglycemia, hyperlipidemia, and oxidative stress in alloxan-treated rats, Mol. Cell. Biochem. 391 (2014) 193–200, https://doi.org/10.1007/s11010-014-2002-x.
[41] A. Abd El Latif, B.E.S. El Bialy, H.D. Mahboub, M.A. Abd Eldaim, *Moringa oleifera* leaf extract ameliorates alloxan-induced diabetes in rats by regeneration of β cells and reduction of pyruvate carboxylase expression, Biochem. Cell Biol. 92 (2014) 413–419, https://doi.org/10.1139/bcb-2014-0081.
[42] S. Verma, M. Gupta, H. Popli, G. Aggarwal, Diabetes mellitus treatment using herbal drugs, International Journal of Phytomedicine 10 (2018) 01, https://doi.org/10.5138/09750185.2181.
[43] A.P. Attanayake, K.A.P.W. Jayatilaka, L.K.B. Mudduwa, C. Pathirana, β-Cell regenerative potential of selected herbal extracts in Alloxan induced diabetic rats, Curr. Drug Discov. Technol. 16 (2019) 278–284, https://doi.org/10.2174/1570163815666180418153024.
[44] S. Jamaddar, A. Raposo, C. Sarkar, U.K. Roy, I.M. Araújo, H.D.M. Coutinho, A. S. Alkhoshaiban, H.A. Alturki, A. Saraiva, C. Carrascosa, M.T. Islam, Ethnomedicinal uses, Phytochemistry, and therapeutic potentials of Litsea glutinosa (Lour.), C. B. Robinson: A Literature-Based Review, Pharmaceuticals 16 (2023), https://doi.org/10.3390/ph16010003.
[45] K. Sukalingam, K. Ganesan, K. Ponnusamy, Evaluation of antidiabetic activity of Polyherbal formulations on type 2 diabetic patients: a single blinded randomized study quick response code, International Journal of Integrative Medical Sciences 2 (2015) 90–98, https://doi.org/10.16965/ijims.
[46] D.J. Marmitt, M.H. Shahrajabian, M.I. Goettert, C. Rempel, Clinical trials with plants in diabetes mellitus therapy: a systematic review, Expert. Rev. Clin. Pharmacol. 14 (2021) 735–747, https://doi.org/10.1080/17512433.2021.1917380.
[47] X. Yao, F. Chen, P. Li, L. Quan, J. Chen, L. Yu, H. Ding, C. Li, L. Chen, Z. Gao, P. Wan, L. Hu, H. Jiang, X. Shen, Natural product vindoline stimulates insulin secretion and efficiently ameliorates glucose homeostasis in diabetic murine models, J. Ethnopharmacol. 150 (2013) 285–297, https://doi.org/10.1016/j.jep.2013.08.043.
[48] Y. Ihara, Y. Yamada, S. Toyokuni, K. Miyawaki, N. Ban, T. Adachi, A. Kuroe, T. Iwakura, A. Kubota, H. Hiai, Y. Seino, Antioxidant α-tocopherol ameliorates glycemic control of GK rats, a model of type 2 diabetes, FEBS Lett. 473 (2000) 24–26, https://doi.org/10.1016/S0014-5793(00)01489-7.
[49] D.K. Semwal, A. Kumar, S. Aswal, A. Chauhan, R.B. Semwal, Protective and therapeutic effects of natural products against diabetes mellitus via regenerating pancreatic β-cells and restoring their dysfunction, Phytother. Res. 35 (2021) 1218–1229, https://doi.org/10.1002/PTR.6885.
[50] S.K. Sadhu, E. Okuyama, H. Fujimoto, M. Ishibashi, E. Yesilada, Prostaglandin inhibitory and antioxidant components of Cistus laurifolius, a Turkish medicinal plant, J. Ethnopharmacol. 108 (2006) 371–378, https://doi.org/10.1016/j.jep.2006.05.024.
[51] Y. Zang, K. Igarashi, Y.L. Li, Anti-diabetic effects of luteolin and luteolin-7-O-glucoside on KK-A(y) mice, Biosci. Biotechnol. Biochem. 80 (2016) 1580–1586, https://doi.org/10.1080/09168451.2015.1116928.
[52] T. Jayakumar, C.Y. Hsieh, J.J. Lee, J.R. Sheu, Experimental and clinical pharmacology of Andrographis paniculata and its major bioactive Phytoconstituent Andrographolide, Evid. Based Complement. Alternat. Med. 2013 (2013) 16, https://doi.org/10.1155/2013/846740.
[53] I.L. Abdulai, S.K. Kwofie, W.S. Gbewonyo, D. Boison, J.B. Puplampu, M. B. Adinortey, Multitargeted effects of Vitexin and Isovitexin on diabetes mellitus and its complications, Sci. World J. 2021 (2021), https://doi.org/10.1155/2021/6641128.
[54] S.T. Assefa, E.Y. Yang, G. Asamenew, H.W. Kim, M.C. Cho, J. Lee, Identification of α-glucosidase inhibitors from leaf extract of pepper (Capsicum spp.) through metabolomic analysis, Metabolites 11 (2021) 649, https://doi.org/10.3390/METABO11100649/S1.
[55] Y. Xu, G. Tang, C. Zhang, N. Wang, Y. Feng, Gallic acid and diabetes mellitus: its association with oxidative stress, Molecules 26 (2021), https://doi.org/10.3390/MOLECULES26237115.
[56] A. Ganogpichayagrai, C. Palanuvej, N. Ruangrungsi, Antidiabetic and anticancer activities of Mangifera indica cv, Okrong leaves, J Adv Pharm Technol Res 8 (2017) 19, https://doi.org/10.4103/2231-4040.197371.
[57] D.J.D. Hartogh, E. Tsiani, Antidiabetic properties of Naringenin: a Citrus fruit polyphenol, Biomolecules 9 (2019), https://doi.org/10.3390/BIOM9030099.
[58] N. Kamaraj, K. Velumani, A. Guru, P.K. Issac, Antihyperglycemic activity of 14-deoxy, 11, 12-didehydro andrographolide on streptozotocin-nicotinamide induced type 2 diabetic rats, Mol. Biol. Rep. 50 (2023) 9875–9886, https://doi.org/10.1007/S11033-023-08878-4.
[59] E.M. Brookes, D.A. Power, Elevated serum urea-to-creatinine ratio is associated with adverse inpatient clinical outcomes in non-end stage chronic kidney disease, Sci. Rep. 12 (2022) 20827, https://doi.org/10.1038/s41598-022-25254-7.
[60] M. Noroozi Karimabad, P. Khalili, F. Ayoobi, A. Esmaeili-Nadimi, C. La Vecchia, Z. Jamali, Serum liver enzymes and diabetes from the Rafsanjan cohort study, BMC Endocr. Disord. 22 (2022) 127, https://doi.org/10.1186/s12902-022-01042-2.
[61] Y. Wang, Y. Liu, H. Wang, C. Li, P. Qi, J. Bao, Agaricus bisporus lectins mediates islet β-cell proliferation through regulation of cell cycle proteins, Exp. Biol. Med. (Maywood) 237 (2012) 287–296, https://doi.org/10.1258/EBM.2011.011251.
[62] J. Cui, J. Duan, J. Chu, C. Guo, M. Xi, Y. Li, Y. Weng, G. Wei, Y. Yin, A. Wen, B. Qiao, Chikusetsu saponin IVa protects pancreatic β cell against intermittent high glucose-induced injury by activating Wnt/β-catenin/TCF7L2 pathway, Aging 12 (2020) 1591–1609, https://doi.org/10.18632/aging.102702.
[63] M. Kawakami, A. Hirayama, K. Tsuchiya, H. Ohgawara, M. Nakamura, K. Umezawa, Promotion of β-cell differentiation by the alkaloid conophylline in porcine pancreatic endocrine cells, Biomed. Pharmacother. 64 (2010) 226–231, https://doi.org/10.1016/j.biopha.2009.09.025.
[64] H. Horiuchi, A. Usami, R. Shirai, N. Harada, S. Ikushiro, T. Sakaki, Y. Nakano, H. Inui, R. Yamaji, S-Equol activates cAMP signaling at the plasma membrane of INS-1 pancreatic β-cells and protects against Streptozotocin-induced hyperglycemia by increasing β-cell function in male mice, J. Nutr. 147 (2017) 1631–1639, https://doi.org/10.3945/jn.117.250860.
[65] L. Ju, X. Wen, C. Wang, Y. Wei, Y. Peng, Y. Ding, L. Feng, L. Shu, Salidroside, a natural antioxidant, improves β-cell survival and function via activating AMPK pathway, Front. Pharmacol. 8 (2017), https://doi.org/10.3389/fphar.2017.00749.
[66] H. Wang, X. He, T. Lei, Y. Liu, G. Huai, M. Sun, S. Deng, H. Yang, R. Tong, Y. Wang, Mangiferin induces islet regeneration in aged mice through regulating p16INK4a, Int. J. Mol. Med. (2018), https://doi.org/10.3892/ijmm.2018.3524.
[67] H. Damame, S. Rooge, R. Patil, C. Garad, A. Arvindekar, *In vitro* differentiation of human pancreatic duct–derived PANC-1 cells into β-cell phenotype using Tinospora cordifolia, In Vitro Cell. Dev. Biol. Anim. 58 (2022) 376–383, https://doi.org/10.1007/s11626-022-00690-x.
[68] T. Tomita, Apoptosis in pancreatic β-islet cells in type 2 diabetes, Bosn. J. Basic Med. Sci. 16 (2016) 162, https://doi.org/10.17305/BJBMS.2016.919.
[69] K. Aamir, H.U. Khan, C.F. Hossain, M.R. Afrin, P.R. Jusuf, I. Waheed, G. Sethi, A. Arya, Arjunolic acid downregulates elevated blood sugar and pro-inflammatory

cytokines in streptozotocin (STZ)-nicotinamide induced type 2 diabetic rats, Life Sci. 289 (2022) 120232, https://doi.org/10.1016/J.LFS.2021.120232.
[70] A. Galli, P. Marciani, A. Marku, S. Ghislanzoni, F. Bertuzzi, R. Rossi, A. Di Giancamillo, M. Castagna, C. Perego, Verbascoside protects pancreatic β-cells against ER-stress, Biomedicines 8 (2020) 582, https://doi.org/10.3390/biomedicines8120582.
[71] A. Mohammed, D. Kumar, S.I. Rizvi, Antidiabetic potential of some less commonly used plants in traditional medicinal systems of India and Nigeria, J Intercult Ethnopharmacol 4 (2015) 78, https://doi.org/10.5455/JICE.20141030015241.
[72] G. Abbas, A. Al Harrasi, H. Hussain, A. Hamaed, C.T. Supuran, The management of diabetes mellitus-imperative role of natural products against dipeptidyl peptidase-4, α-glucosidase and sodium-dependent glucose co-transporter 2 (SGLT2), Bioorg. Chem. 86 (2019) 305–315, https://doi.org/10.1016/j.bioorg.2019.02.009.
[73] J. Yoshida, Y. Okawa, T. Oyama, N. Shimoda, S. Uesugi, H. Takagi, Y. Ito, K. Ichi Kimura, Inhibition of Calcineurin and glycogen synthase kinase-3β by Ricinoleic acid derived from Castor oil, Lipids 55 (2020) 89–99, https://doi.org/10.1002/LIPD.12208.
[74] A.S.D. Wickramasinghe, P. Kalansuriya, A.P. Attanayake, Herbal medicines targeting the improved β-cell functions and β-cell regeneration for the Management of Diabetes Mellitus, Evid. Based Complement. Alternat. Med. 2021 (2021) 1–32, https://doi.org/10.1155/2021/2920530.
[75] F. Rabizadeh, M.S. Mirian, R. Doosti, R. Kiani-Anbouhi, E. Eftekhari, Phytochemical classification of medicinal plants used in the treatment of kidney disease based on traditional Persian medicine, Evid. Based Complement. Alternat. Med. 2022 (2022), https://doi.org/10.1155/2022/8022599.
[76] B. Ansarullah, M. Bharucha, M. Umarani, N.C. Dwivedi, R. Laddha, A.A. Begum, A. V. Hardikar, Ramachandran, *Oreocnide integrifolia* flavonoids augment reprogramming for islet Neogenesis and *β* -cell regeneration in Pancreatectomized BALB/c mice, Evid. Based Complement. Alternat. Med. 2012 (2012) 1–13, https://doi.org/10.1155/2012/260467.
[77] N. Fatima, R.M. Hafizur, A. Hameed, S. Ahmed, M. Nisar, N. Kabir, Ellagic acid in Emblica officinalis exerts anti-diabetic activity through the action on β-cells of pancreas, Eur. J. Nutr. 56 (2017) 591–601, https://doi.org/10.1007/S00394-015-1103-Y.
[78] L. Guasch, E. Sala, M.J. Ojeda, C. Valls, C. Bladé, M. Mulero, M. Blay, A. Ardévol, S. Garcia-Vallvé, G. Pujadas, Identification of Novel Human Dipeptidyl Peptidase-IV Inhibitors of Natural Origin (Part II): *In Silico* Prediction in Antidiabetic Extracts, PLoS One 7, 2012, https://doi.org/10.1371/JOURNAL.PONE.0044972.
[79] A.O. Abdel-Zaher, I.T. Ahmed, A.E.D.A. El-Koussi, The potential antidiabetic activity of some alpha-2 adrenoceptor antagonists, Pharmacol. Res. 44 (2001) 397–409, https://doi.org/10.1006/phrs.2001.0870.
[80] G.C. Wang, Y. Wang, I.D. Williams, H.H.Y. Sung, X.Q. Zhang, D.M. Zhang, R. W. Jiang, X.S. Yao, W.C. Ye, Andrographolactone, a unique diterpene from Andrographis paniculata, Tetrahedron Lett. 50 (2009) 4824–4826, https://doi.org/10.1016/J.TETLET.2009.05.097.
[81] P.C. Lekshmi, R. Arimboor, P.S. Indulekha, A. Nirmala Menon, Turmeric (Curcuma longa L.) volatile oil inhibits key enzymes linked to type 2 diabetes, Int. J. Food Sci. Nutr. 63 (2012) 832–834, https://doi.org/10.3109/09637486.2011.607156.
[82] G.D. Bae, E.Y. Park, D.J. Baek, H.S. Jun, O. Yoon Sin, Liquiritigenin prevents palmitate-induced beta-cell apoptosis via estrogen receptor-mediated AKT activation, Biomed. Pharmacother. 101 (2018) 348–354, https://doi.org/10.1016/J.BIOPHA.2018.02.097.
[83] H.A. Zhang, D.D. Kitts, Turmeric and its bioactive constituents trigger cell signaling mechanisms that protect against diabetes and cardiovascular diseases, Mol. Cell. Biochem. 476 (2021) 3785, https://doi.org/10.1007/S11010-021-04201-6.
[84] S. Bakrim, N. Benkhaira, I. Bourais, T. Benali, L.H. Lee, N. El Omari, R.A. Sheikh, K. W. Goh, L.C. Ming, A. Bouyahya, Health benefits and pharmacological properties of Stigmasterol, Antioxidants 11 (2022) 1912, https://doi.org/10.3390/ANTIOX11101912.
[85] A.H. Mohammed, S.Z. Na'inna, M. Yusha'u, B. Salisu, U. Adamu, S.A. Garba, Phytochemical screening and antibacterial activity of Mangifera indica extracts, UMYU Journal of Microbiology Research (UJMR) 1 (2016) 23–28, https://doi.org/10.47430/UJMR.1611.004.
[86] T. Jayakumar, C.Y. Hsieh, J.J. Lee, J.R. Sheu, Experimental and clinical pharmacology of Andrographis paniculata and its major bioactive Phytoconstituent Andrographolide, Evid. Based Complement. Alternat. Med. 2013 (2013) 16, https://doi.org/10.1155/2013/846740.
[87] S. Meng, J. Cao, Q. Feng, J. Peng, Y. Hu, Roles of Chlorogenic acid on regulating glucose and lipids metabolism: a review, Evid. Based Complement. Alternat. Med. 2013 (2013) 801457, https://doi.org/10.1155/2013/801457.
[88] B. Salehi, A. Venditti, M. Sharifi-Rad, D. Kręgiel, J. Sharifi-Rad, A. Durazzo, M. Lucarini, A. Santini, E.B. Souto, E. Novellino, H. Antolak, E. Azzini, W.N. Setzer, N. Martins, The therapeutic potential of Apigenin, Int. J. Mol. Sci. 20 (2019), https://doi.org/10.3390/IJMS20061305.
[89] N. Suemanotham, S. Phochantachinda, D. Chatchaisak, W. Sakcamduang, A. Chansawhang, P. Pitchakarn, B. Chantong, Antidiabetic effects of Andrographis paniculata supplementation on biochemical parameters, inflammatory responses, and oxidative stress in canine diabetes, Front. Pharmacol. 14 (2023) 1077228, https://doi.org/10.3389/FPHAR.2023.1077228/BIBTEX.
[90] R.S. Shenoy, K.V.H. Prashanth, H.K. Manonmani, *In vitro* antidiabetic effects of isolated triterpene glycoside fraction from Gymnema sylvestre, Evid. Based Complement. Alternat. Med. 2018 (2018), https://doi.org/10.1155/2018/7154702.
[91] A.E. Al-Snafi, A.E. Al, Pharmacology and medicinal properties of *Caesalpinia crista*-An overview. www.ijpjournal.org, 2015.
[92] D.T. Trang, B.H. Tai, N.H. Hoang, N.T. Cuc, N.A. Bang, D.T. Dung, D.T.H. Yen, P.T. T. Huong, N.V. Dung, D.T.T. Hang, P.H. Yen, P. Van Kiem, Undescribed triterpenes from the leaves of Syzygium myrsinifolium with their α-glucosidase and α-amylase inhibition activity, Chem. Biodivers. 21 (2024), https://doi.org/10.1002/CBDV.202400124.
[93] G. Jonathan, R. Rivka, S. Avinoam, H. Lumír, B. Nirit, Hypoglycemic activity of withanolides and elicitated Withania somnifera, Phytochemistry 116 (2015) 283–289, https://doi.org/10.1016/J.PHYTOCHEM.2015.02.029.
[94] B. Dallaqua, F.H. Saito, T. Rodrigues, I.M.P. Calderon, M.V.C. Rudge, E. Herrera, D. C. Damasceno, Treatment with Azadirachta indica in diabetic pregnant rats: negative effects on maternal outcome, J. Ethnopharmacol. 143 (2012) 805–811, https://doi.org/10.1016/J.JEP.2012.07.023.
[95] S. Un, N. Van Quan, L.H. Anh, V.Q. Lam, A. Takami, T.D. Khanh, T.D. Xuan, Effects of *In Vitro* Digestion on Anti-α-Amylase and Cytotoxic Potentials of Sargassum spp., Molecules 2022, Vol. 27, Page 2307 27, 2022, p. 2307, https://doi.org/10.3390/MOLECULES27072307.